

Soil Sensors and Plant Wearables for Smart and Precision Agriculture

Heyu Yin, Yunteng Cao, Benedetto Marelli, Xiangqun Zeng, Andrew J. Mason, and Changyong Cao*

Soil sensors and plant wearables play a critical role in smart and precision agriculture via monitoring real-time physical and chemical signals in the soil, such as temperature, moisture, pH, and pollutants and providing key information to optimize crop growth circumstances, fight against biotic and abiotic stresses, and enhance crop yields. Herein, the recent advances of the important soil sensors in agricultural applications, including temperature sensors, moisture sensors, organic matter compounds sensors, pH sensors, insect/pest sensors, and soil pollutant sensors are reviewed. Major sensing technologies, designs, performance, and pros and cons of each sensor category are highlighted. Emerging technologies such as plant wearables and wireless sensor networks are also discussed in terms of their applications in precision agriculture. The research directions and challenges of soil sensors and intelligent agriculture are finally presented.

1. Introduction

Agriculture is the main source of food grains and many other widely used raw materials (e.g., wool, crop stalks), and a key driving force of economic transformation and growth.^[1,2] Increasing agricultural productivity and incomes is crucial to reducing poverty and achieving food security.^[3] With around 820 million people across the globe being undernourished and a 34% projected growth of world population by 2050—corresponding to a 60% increase in food demand—there is

a compelling need to utilize advanced technologies in the agriculture sector to increase agricultural productivity and reduce food losses to guarantee food security.^[2] In this regard, “smart agriculture” or “precision agriculture” has been attracting increasing attention due to its capability for using less to grow more compared to traditional agricultural practices. In addition, it improves the quality of the work environment and social aspects of farming, ranching, and other relevant professions.^[4]

Smart agriculture comprises a set of technologies that combines sensors, information systems, enhanced machinery, and informed management to optimize production by accounting for variabilities

and uncertainties within sustainable agricultural systems.^[3–5] Among the set of technologies, advanced sensing systems that monitor soil health and conditions and crop developments are of paramount importance because they collect and evaluate critical data for decision making and management, especially when crop growth conditions vary considerably over space and time. Spatial variation may result from soil properties, diseases, weeds, pests, and previous land management. In particular, some soil properties (e.g., moisture, pH, nutrients) and plant diseases may form long-term spatial patterns. Temporal variability arises from weather patterns and management practices. In summary, the soil properties relevant to crop growth include a range of soil conditions including soil gas, moisture, temperature, nutrients, pH, and pollutants in the soil (Figure 1).^[6,7]

Monitoring the soil conditions will provide key information not only to improve resource utilization to maximize farming outputs and minimize environmental side effects but also to build site-specific databases of relationships between soil conditions and plant growth for intelligent and sustainable agriculture systems. Traditionally, soil properties are measured by soil sampling and offsite laboratory analysis or by on-site measurement to provide an extensive knowledge of soil information.^[8] Seasonally varying crop growth conditions, such as water stress, lack of nutrients, diseases, weeds, and insects, are evaluated by visual inspection and laboratory analysis of plant tissues. The relatively periodically coarse sampling/measurement rate of these conventional strategies may not be sufficient to reveal variation at the appropriate spatial and temporal resolution. Novel technologies for collecting soil information with sufficient spatiotemporal resolutions are in demand to build efficient smart or precision agriculture systems. With the

H. Yin, Prof. A. J. Mason, Prof. C. Cao
 Department of Electrical and Computer Engineering

Michigan State University
 East Lansing, MI 48824, USA
 E-mail: ccao@msu.edu

H. Yin, Prof. C. Cao
 Laboratory for Soft Machines & Electronics
 School of Packaging
 Michigan State University
 E-mail: East Lansing, MI 48824, USA

Y. Cao, Prof. B. Marelli
 Department of Civil and Environmental Engineering
 Massachusetts Institute of Technology
 Cambridge, MA 02139, USA

Prof. X. Zeng
 Department of Chemistry
 Oakland University
 Rochester, MI 48309, USA

 The ORCID identification number(s) for the author(s) of this article can be found under <https://doi.org/10.1002/adma.202007764>.

DOI: 10.1002/adma.202007764

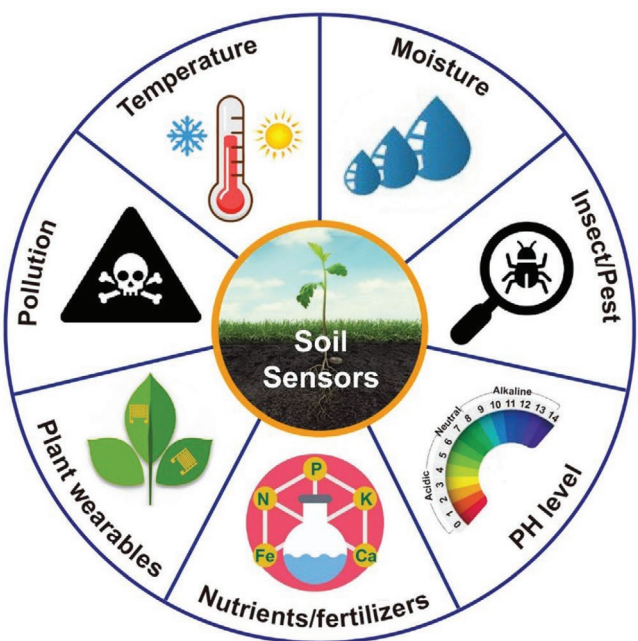


Figure 1. The major sensors for detecting health conditions of soil in smart agriculture. These sensors include soil moisture sensors, soil temperature sensors, soil pH sensors, soil nutrient sensors, soil pest/insect sensors, soil pollution sensors, and plant wearables. For each type of the sensors, we will discuss the significant progress of sensor designs, sensing technologies, device performance, pros and cons, and fabrication.

development of sensing and wireless communication technologies, remote and in situ monitoring the physical, chemical, and biological attributes of soil (e.g., moisture content, salinity, temperature, pH level, nutrients) is becoming possible and will enable the development of advanced smart agriculture systems.

Here, we summarize recent advances regarding different types of soil sensors, plant wearables, as well as the development of sensor network systems implemented for smart and precision agriculture applications, with an emphasis on several key sensor factors in monitoring signals within the plant growth cycles. As shown in Figure 1, within the crop's micro-environment, soil moisture level, temperature, pH variation, nutrient elements, pests/insects, and soil pollutants are key elements that determine the crop productivity. Site-specific agriculture management, such as the necessity and quantity of irrigation, fertilizers, and pesticides, will depend on the soil condition data collected using different kinds of soil sensors. Soil sensors, including the six different kinds of soil sensors that measure the soil properties directly, and sensor network systems that include underground sensors and plant wearables to evaluate the soil and plant health, are systematically reviewed and discussed. We highlight the major technologies, designs, performance, and pros and cons of each kind of sensor. Particularly, we discuss the self-powered wireless sensor networks for the implementation of smart and precision agriculture systems. The research trends and challenges of soil sensors and intelligent agriculture are finally presented for guiding future study.

2. Advances of Typical Soil Sensors

2.1. Soil Moisture Sensors

Soil moisture, also known as soil water, is an important parameter for soil health evaluation and plays a key role in plant growth. It is the water source for crops to maintain their physiological activities. Soil moisture level significantly influences the physicochemical properties of soil, thus affecting salt dissolution, plants' uptakes of water and ions, and microbial activities. Therefore, monitoring soil moisture level is of great significance to maintain suitable soil conditions for agriculture production. Soil moisture sensors are used to estimate the water content in soil, based on which farmers are informed the irrigation time and amount at a proper level for plant growth.^[9]

Typically soil moisture sensors are composed of three parts: the probe electrodes embedded in soil to supply bias and readout, the transmission circuits (e.g., coaxial cables), and the electronics or instruments for signal processing (Figure 2a). To determine the water content in soil, current soil moisture sensors are measuring the changes of soil properties related to water content,^[10] such as the dielectric permittivity, matric potential, and mass (volumetric water content) of soils.^[8] Soil moisture sensors can be categorized by their working mechanisms into four groups: capacitive-based moisture sensors,^[11–13] electro-magnetic induction (EMI)-based moisture sensors, ultrasonic-based moisture sensors,^[9] and optical sensors. The capacitive-based moisture sensor is the most widely used soil moisture sensing technology, which measures the capacitance with no exposed metal. In contrast, the EMI approaches are operated at low frequencies (e.g., 38 kHz for EM38 model) with wide horizontal separation between coils, avoiding the troublesome issues in drilling cores and down-tube installations.^[14–16] Although EMI approaches have demonstrated major advantages, such as rapid measurement, high accuracy, easy access to deep soil layers, the high-cost and low resistance to interference affected its use for smart agriculture applications. Ultrasonic-based soil sensors measure the acoustic impedances difference between forward and back ultrasonic waves to categorize the moisture level, which are usually more expensive due to the requirement of ultrasonic source and integrated detector. Any change of the water content will be reflected through the calculated difference between back-and-forth signals of the ultrasonic soil sensor.

The apparent permittivity (or dielectric constant) of soil is directly related to its moisture content.^[17] The change of the moisture content in soil will induce dramatically dielectric permittivity change (Figure 2a).^[8,10,18] Compared to other approaches like tensiometers,^[19,20] techniques based on the measurement of dielectric constant easily overcome the restriction of climatic conditions and be more suitable for continuous monitoring. For example, Dean et al. developed low-cost small-scale interdigitated capacitive sensors for soil moisture measurement based on micro-electro-mechanical system (MEMS) and printed circuit board technologies (Figure 2b).^[21] The as-fabricated capacitive sensors showed a nearly linear relationship between the measured capacitance and soil moisture content because the dielectric constant of soil varies in proportion to moisture content.^[22] Sulaiman et al. designed a fringing electric field moisture sensor capable of detecting moisture from

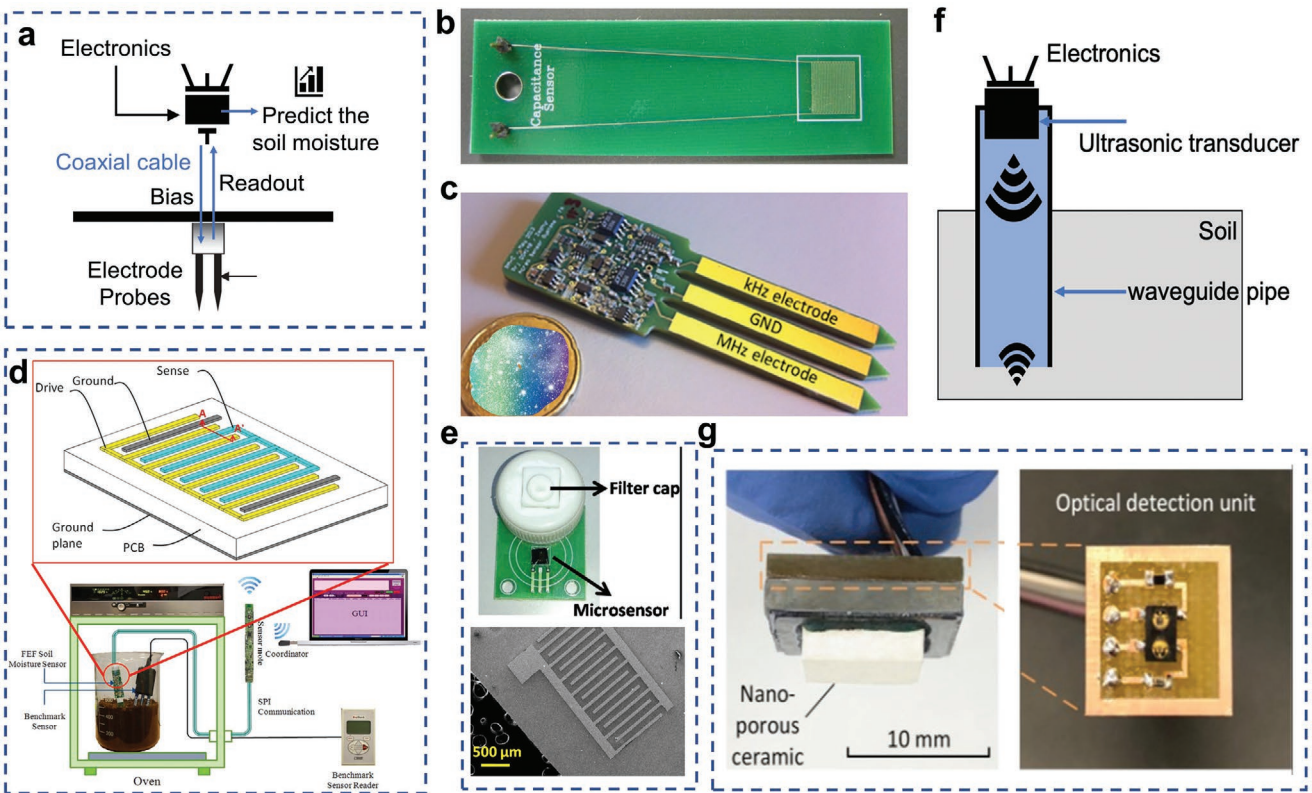


Figure 2. Soil moisture sensors. a) Schematic illustration of a typical soil moisture sensor with critical components. b) Photograph of the prototype of a capacitance soil moisture sensor. c) Photograph of a miniaturized wireless system for sensing soil water content and conductivity. d) Schematic diagram and test setup for a volumetric soil moisture sensor. e) Graphene quantum dot (GQD) soil moisture sensor packaged with a filter cap. SEM image of the IDE with dimensions of $1.5\text{ mm} \times 2.4\text{ mm}$. f) Schematic design of an ultrasonic soil moisture sensor. g) A miniaturized optical moisture sensor for direct, continuous, in situ monitoring soil water potential variations through the nanoporous ceramic diaphragm. b) Reproduced with permission.^[21] Copyright 2012, IEEE. c) Reproduced with permission.^[40] Copyright 2019, IOP Publishing. d) Reproduced with permission.^[13] Copyright 2009, IEEE. e) Reproduced with permission.^[44] Copyright 2016, IEEE. g) Reproduced with permission.^[50] Copyright 2019, IEEE.

1% to 80% volumetric water content with a linear response (Figure 2d).^[13] The measured capacitance from the sensor was connected directly to the device input using capacitance to digital converter, and wirelessly transferred using the Zigbee technology (Figure 2d). One major drawback of the sensor is the small penetration depth due to the small size of the sensor and the error readings due to the variability of the electrode thickness and geometry.

Time-domain reflectometry (TDR) measures the dielectric constant of soil via the propagation velocity of a pulse travelling along the electromagnetic transmission line embedded in the soil. Using TDR, Davis et al. empirically determined the dependence of the dielectric constant, at frequencies between 1 MHz and 1 GHz, on the volumetric water content to measure the dielectric constant of a wide range of granular specimens.^[23] They concluded that the soil dielectric constant is strongly dependent on the volumetric water content and is almost independent of soil density, texture, salt content, and even temperature. With the same TDR technology, more groups are studying how to design the transmission line, how to perform calibration, how to relate ionic conductivity with frequency, and how to take into account temperature influence.^[24–29] Time domain transmissometry (TDT) is another dielectric constant measurement technology which measures

electromagnetic wave propagation time in one direction over the length of the probe.^[30–32] In contrast with TDR, TDT measures the transmission of a pulse along a closed circuit or looped rod, reporting enhanced accuracy benefiting from its robustness against multiple reflections along the sensor.^[33] In the frequency domain reflectometry, the frequency change of the electromagnetic wave between output wave and the return wave is measured to evaluate the soil moisture.^[34] Ground penetrating radar uses the transmission and reflection of high frequency (1 GHz) electromagnetic waves within the subsurface to measure the soil's dielectric constant.^[35,36] However, this type of technique is not only suffering from bulky and expensive instruments, but also complex signal processing due to signal attenuation. Campbell developed a network analyzer and a coaxial-transmission-line type of dielectric probe to measure the complex, dielectric response (both real and imaginary) of soil.^[24] Their dielectric probe measured the ratio of reflected voltage to an incident voltage signal with frequency range from 1 to 50 MHz, dependent on the impedance of the medium between the probes. The imaginary dielectric constant showed variation between soils due to an ionic-conductivity loss mechanism, while the real dielectric constants of soils clearly exhibited direct correlation with water content at the frequency of 50 MHz.

Differing from the TDR technology, Gaskin and Miller reported a simplified impedance measuring system with a probe structure design to determine soil water content.^[37] Their impedance probe consisted of a resistor, a coaxial transmission line, and a stainless-steel wire soil sensing probe. The volumetric moisture fraction exhibited a cubic relationship with the voltage on a load resistor. However, this impedance measuring system depended on temperature and salinity. The bulk electrical conductivity of moist soil is influenced by the electrical conductivity of pore water, the water concentrations, the tortuosity of electrical flow paths in soil matrix, and the series coupled surface conductivity of soil particles.^[38,39] As shown in Figure 2c, Rusu et al. developed a miniaturized wireless water content and conductivity soil sensor system based on measuring the frequency-dependent electrical conductivity.^[40] For nonswelling soils (swelling pressure < 0.15 kg cm⁻²), the change in volumetric heat capacity is primarily due to the change of soil moisture.^[41,42] Thus, volumetric heat capacity can be utilized to characterize the soil moisture. A dual-probe heat capacity sensor consisting of a heater and a temperature sensor was fabricated to measure the volumetric water content.^[43] The temperature change induced by the instantaneous pulses generated by a line heater at a short distance is inversely related to the soil volumetric heat capacity determined by the volumetric moisture content. Kalita et al. proposed a resistive type of soil moisture sensor (Figure 2e) using graphene quantum dots (GQDs) that demonstrated a response time of 120–180 s and good stability of 4 months.^[44] They fabricated gold (Au) interdigitated electrodes (IDE) on a Si wafer using a photolithography process while the electrochemically synthesized GQDs were drop-casted on the IDE as a sensing material. A sensirion (SHT1X) filter cap was used to package the sensor, which allowed only soil moisture to diffuse inside the chamber and interact with IDE micro-sensor. The adsorption of water molecules coming from the soil surface onto the GQDs surface strengthened the coupling between the dots, thereby increasing the conductivity.

Figure 2f illustrates an ultrasonic detector consisting of a brass or stainless-steel waveguide pipe and an ultrasonic transducer fixed on the upper part of the pipe.^[45] An ultrasonic wave of 40 kHz generated by the transducer and the reflection mode of the ultrasonic waves was compared to record the scattering effect at the surface of the underground soil, which depended on the soil moisture content. This ultrasonic detector can be easily installed underground for multipoint monitoring in a wide field area. However, the temperature-dependent effect of such ultrasonic sensors must be corrected using a dummy pair system since the measurement data are greatly influenced by temperature. In addition, compare to commonly used capacitive soil moisture sensors (e.g., Adafruit STEMMA soil sensor, sold as only \$7.5), ultrasonic sensors that are now commercially available are much more expensive (e.g., UGT582 sensor, sold as \$173), hindering their widely deployment in smart agriculture systems.

Optical methods, such visible and near-infrared (NIR) spectrophotometers, have also been broadly utilized to perform online soil moisture measurement. Moisture absorption bands exist in the NIR wavelength (1450, 1940, 2950 nm),^[46] therefore, the reflection spectrum variation appears when the moisture

molecular absorption of the light changes.^[47–49] Recently, Dong et al. developed a miniature embedded sensor for direct, continuous, in situ monitoring of soil water potential variations (Figure 2g).^[50] The soil moisture change in the surrounding environment will affect the moisture level in the water reservoir covered by a nanoporous ceramic membrane, which will then bend the SiO₂–Si diaphragm into the reservoir due to an induced negative pressure. By increasing the hydrophilicity and smoothness of the SiO₂–Si diaphragm, a high cavitation pressure was obtained to enable a high resolution (\approx 0.04 kPa) of the device.

2.2. Soil Temperature Sensors

Soil temperature, ranging from –10 to 50 °C,^[51] is an important parameter for agriculture because it influences germination, blooming, composting, and a variety of plant growth processes, and also significantly influences the physical, chemical, and microbiological processes in soils that play critical roles in plant growth.^[52,53] Soil temperature is strongly affected by soil properties including specific heat capacity, thermal conductivity, bulk density, texture, water content, and surface covering materials.^[54,55] As shown in Figure 3a, a soil temperature sensor consists of the temperature probes to transfer the temperature variation into electrical signal and the bias and readout electronics to interpret the electrical signal into digital data.^[55] There are many electronic temperature sensors that can be used as soil temperature sensors, including thermocouples, resistance temperature detectors (RTDs), thermistors, and semiconductor-based temperature sensors.^[56–59]

Thermocouples use the electrical potential generated by a pair of thermoelectrically dissimilar metal/conductor junctions, commonly iron/constantan, to obtain a millivolt reading which can be translated to temperature. Thermocouples can be used for precise monitoring of soil temperature due to their fast response to sudden changes in temperature and ease of automation.^[60] When used for long-distance measurement, thermocouples require long cables with good match resistance and specific calibration of the system for accurate measurements.^[55] RTDs are typically made of a metal conductive wire wrapped around a ceramic or glass core. The soil temperature can be recorded by measuring the voltage across the RTD with a constant current bias. Compared to thermocouples, RTDs have higher accuracy, better stability, and better repeatability in temperature measurements.^[61,62] However, RTDs are usually fragile and have to be protected in the probes, leading to extra resistance to temperature variation. Different from RTDs, thermistors are constructed with ceramic semiconductors or polymers instead of metal. Thermistors have either a positive temperature coefficient, or a negative temperature coefficient. Since ceramic semiconductors typically have larger thermal coefficients, thermistors can provide better resolutions compared to RTDs. However, the temperature-resistance relationship may be nonlinear, which requires a complicated calibration process. Linear thermistor networks connecting several thermistors in series or in parallel can be developed to solve the nonlinear problem, but may induce higher costs.^[63–65]

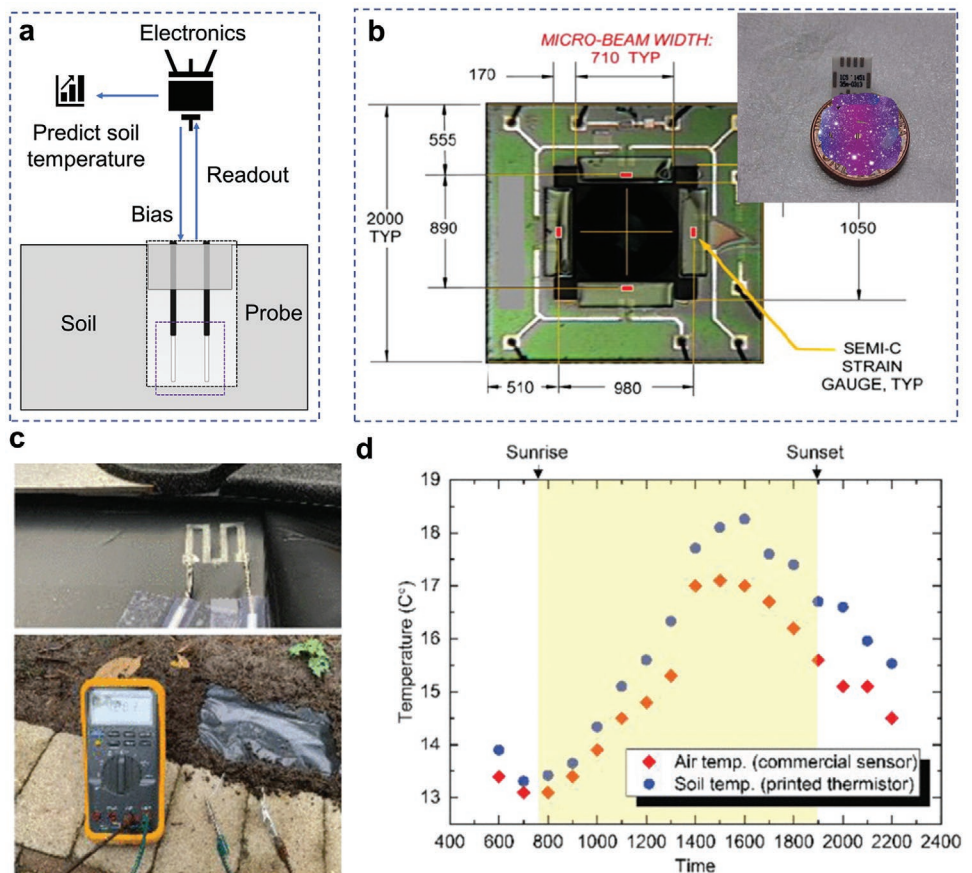


Figure 3. Soil temperature sensors. a) Schematic diagram of a soil temperature sensor. b) An on-chip MEMS thin-film polymer sensor for soil moisture sensing and an on-chip piezoresistor for soil temperature monitoring. The inset shows the packaged MEMS sensor. c) Measurement setup and d) test results using a biodegradable soil temperature sensor made from an inkjet-printed thermistor on a biodegradable PE mulch film. a,b) Reproduced with permission.^[66] Copyright 2008, Elsevier. c,d) Reproduced with permission.^[63] Copyright 2019, IEEE.

Utilizing the temperature sensitivity of P-N junction, the bipolar transistor can generate a voltage signal across the base and emitter with a constant current bias. The thermal coefficient is typically $-2 \text{ mV } ^\circ\text{C}^{-1}$, a higher resolution and better linearity compared to thermocouples and RTDs. Since the silicon-based temperature sensor is more compatible with IC circuits, better performance regarding soil monitoring can be achieved when integrated with an IC circuitry. The only concern is the variation of the manufacturing process with both the temperature sensor and IC circuitry, which in return makes the calibration unavoidable. One representative example is a recent on-chip piezoresistive (thermistor) temperature sensor developed by Jackson et al. (Figure 3b).^[66] Their thermistor was bonded onto a silicon-based MEMS chip to measure temperature. The temperature sensitive piezoresistor was fabricated by depositing a doped semiconductor strain gauge on top of the cantilever. The soil temperature variation is sensed by measuring the resistance change due to the thermal expansion of the piezoresistor.^[66] Recently, Sui et al. also fabricated a silver-based biocompatible soil temperature sensor through a low temperature inkjet-printing protocol (Figure 3c), and the sensor demonstrated an average sensitivity of $0.246 \Omega \text{ } ^\circ\text{C}^{-1}$, independent of substrate materials.^[63]

2.3. Soil pH Sensors

Soil pH is a measure of the acidity or basicity/alkalinity of soil, reflecting the combined effects of the soil-forming factors such as parent material, organisms, and climate. Besides its influence on microbial activities, soil pH determines the chemical forms of different nutrients thus affects plant nutrient availability. The optimal pH range of soil suitable for growth of most plants is between 5.5 and 7.5.^[67] For smart and precision agriculture, pH value of soil can provide valuable information for controlling the health of soil in a suitable range for specific crops in the farm.

A few sensing technologies are used for soil pH evaluation: optical (e.g., colorimetric or photometric methods), electrochemical (e.g., conductometric and potentiometric methods), and acoustic methods.^[68,69] Colorimetric and photometric indicators, such as dyes and pH test strips, rely on color changes of specific organic pigments that are sensitive to pH, and necessary pH-color charts are used to read the pH level. Compare to colorimetric methods, photometric methods,^[68] such as optical fiber pH sensors,^[70,71] fluorometric pH sensors,^[72] holographic pH sensors,^[72,73] as well as CCD camera full range pH sensors,^[74] provide much higher resolution and accuracy. However, due to the complex optical system, none of them is

suitable for in-site soil measurements. As shown in Figure 4a, a typical conductometric pH sensor consists of conductivity electrodes and a thin layer of pH-responsive sensing material. The shrinking of the hydrogel sensing layer causes a response to the analyst, thereby resulting in the change of electrical properties. The conductometric pH sensor was fabricated by coating an interdigitated electrode (IDE) with a pH-sensitive hydrogel membrane.^[75,76] A reversely pH-dependent swelling hydrogel could be used for such a design to build reusable pH sensors.^[77] However, due to the use of a hydrogel sensing layer, a soil solution had to be prepared for the pH monitoring. To overcome this limitation, a new type of pH-sensitive polymer materials (adjustable ion concentration and hence conductivity) was developed to make the in situ soil conductometric sensor available.^[78] Drop-coating polyaniline/polyvinyl butyral onto the IDEs could increase the adhesion between the pH-sensitive film and the electrode/substrate.^[79] Tin oxides (SnO_2 and SnO) and TiO_2 were explored as a sensing layer to replace hydrogel, and the obtained SnO_2 -based pH sensor demonstrated considerable pH-conductivity relationship at low working frequencies.^[80,81]

Figure 4b presents a potentiometric soil pH sensor composed of sensing half-cell (i.e., ion-selective electrodes, the potential directly related to the pH value of the sample) and reference half-cell (providing the stable reference electrode potential value).^[82] This sensor structure needs two separated electrodes, one is coated with a pH-sensitive material (e.g., pH-sensitive glass), the other is made of an inert material (e.g., Ag/AgCl) to serve as the reference electrode. The pH value is obtained by comparing the potential difference between the two cells. The potentiometric soil pH sensing cell was made of a

glass electrode with an Ag/AgCl wire and electrolyte inside.^[67] In the reference half-cell, Ag/AgCl with a salt solution with a constant concentration of Cl^- can provide very stable reference potential, while in the sensing half-cell, the inside of the ion-sensitive glass membrane is filled with hydrochloric acid (HCl) at a known proton concentration. The pH changes, due to the variation of H^+ at the two sides of the glass membrane, can be measured based on Nernst equation because the pH value is directly related to the glass membrane potential. Because the glass electrode is fragile, other materials have been studied to replace the proton-sensitive glass. Having its basis on benzoxazole guanidine (BG) as a suitable ionophore, a polyvinyl chloride (PVC) membrane electrode for dysprosium (III) ions was built to replace the proton-selective glass membrane. With the replaced membrane, noticeable potential divergence and good selectivity with respect to most alkali in soil were reported.^[83] Compared to PVC, a pH-sensitive membrane based on a photocurable urethane-acrylate polymer with dictyoseptate as plasticizer and tetra-dodecyl-amine as ionophore was easily fabricated.^[84] The pH-sensitive membrane based on ion-selective electrodes demonstrated a sensitivity of 55 mV per pH and a linear range of pH from 2 to 10.

In addition, the performance of ion-selective pH sensors can also be improved through electrode material modification and new fabrication methods (Figure 4c). For example, by depositing thin films of $\alpha\text{-PbO}_2$ and $\beta\text{-PbO}_2$ on aluminum substrate electrodes, the modified ion-selective electrodes exhibited potentiometric response to hydrogen ion concentration.^[85] The potentiometric response of the modified electrodes was approaching the theoretical slope of Nernstian response and

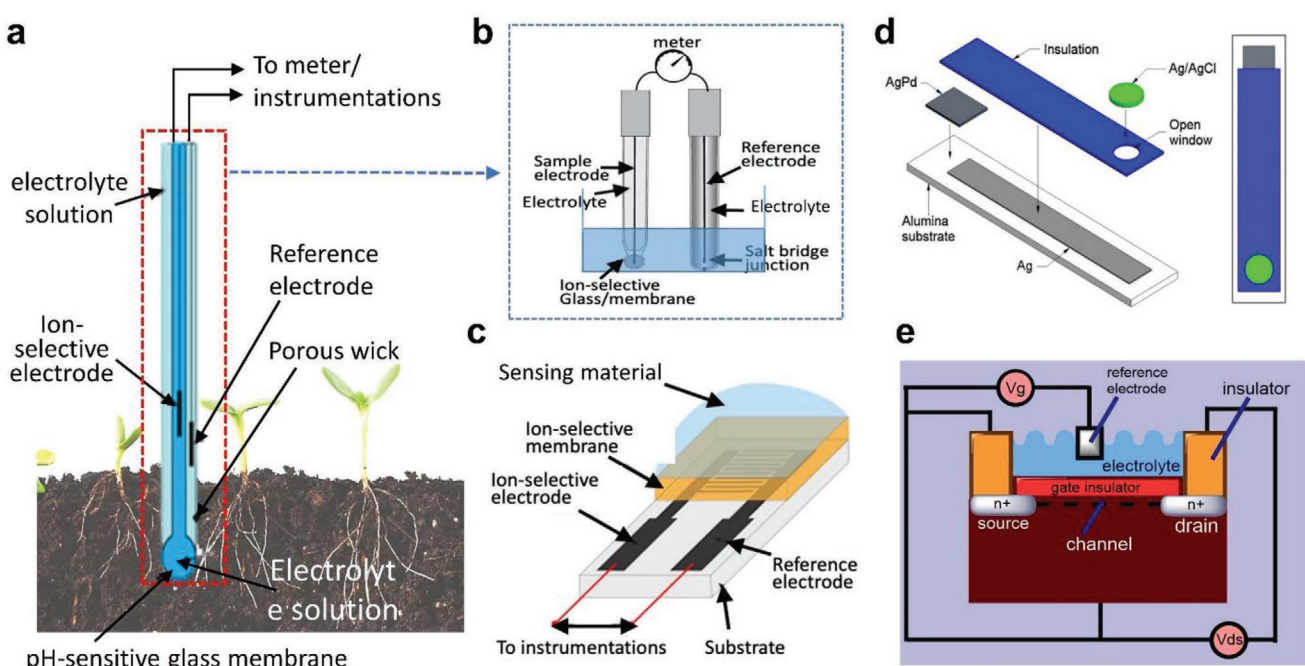


Figure 4. Soil pH sensors. a) Schematic illustration of a soil pH sensor. b) A potentiometric soil pH sensor consisting of a sensing half-cell and a reference half-cell. c) Schematic of a pH sensing layer made of interdigitated ion-selective electrode structure with an ion-selective membrane. d) Screen-printed ion-selective electrodes for pH sensing. e) Schematic illustration of an ISFET structure for soil pH detection. a,b) Reproduced with permission.^[82] Copyright 1974, American Chemical Society. d) Reproduced with permission.^[86] Copyright 2011, Elsevier. e) Reproduced with permission.^[89] Copyright 2011, Elsevier.

comparable with that of the glass pH electrodes.^[85] As shown in Figure 4d, researchers employed screen-printing methods to fabricate electrochemical pH sensors. The mechanical and chemical robustness of the printed electrodes were validated through the detection of pH and salinity change when immersed in soil columns. These screen-printed sensors can serve as an invaluable tool for hydrology, agricultural science, soil science, and environmental science.^[86]

Ion selective field effect transistor (ISFET) is an alternative for soil pH sensing.^[68,69,87,88] An ISFET consists of a drain electrode and a source electrode together with a third gate electrode between them (Figure 4e). pH-sensitive materials, such as silicon oxide (SiO_2), silicon nitride (Si_3N_4), and aluminum oxide can be coated on top of the gate electrode. When an ISFET is exposed to the testing solution, the pH-responsive material will induce a change of the gate voltage, thereby the current from source to drain electrode will vary based on the pH change. Compared to the ion-selective electrodes, the ISFET is more compatible with the advanced IC design, which in return can provide advantages such as miniaturization, system integration, excellent sensitivity, and resolution, as well as good stability and selectivity.^[88–90] However, due to the complexity of the soil environment, ISFETs need to be packed very well to avoid any damage when inserted into the soil.

Bashir and Gupta designed a microcantilever-based pH sensor,^[91] in which the cantilever was fixed on top of a piezoresistive hydrogel or polymer layer. When the pH changes in the test solution, the hydrogel/polymer layer will shrink or swell, leading to the deformation of the cantilever. Thus, the pH value of the test sample can be reported by measuring the frequency change induced by the cantilever deformation.^[68,91] Modified silicon (SiO_2)/(Si_3N_4) was used as the micro-cantilever for pH measurement via the micromechanical technique.^[92] For example, an aminosilane-modified SiO_2/Au cantilever performs robustly over pH range 2 ± 8 (49 nm detection/pH unit), while $\text{Si}_3\text{N}_4/\text{Au}$ cantilevers perform well at pH 2 ± 6 and 8 ± 12 (30 nm detection/pH unit). The cantilever-based pH sensor shows a high sensitivity, but the system is more complex and quite sensitive to noise. Recently, a magnetoelastic pH sensor was proposed to address this issue.^[93] In the new design, when an electrical field was applied to the driving coil, the induced magnetic field enforced the substrate to vibrate at a certain frequency. The mass (swelling or shrinking) of the pH-sensitive material changed with the pH value. Then, the induced mass variation of the sensitive material affected the vibration frequency. As a result, the pH change can be calculated based on the interconversion between the magnetic energy and the elastic energy.

2.4. Soil Nutrient Sensors

Among the soil organic matters (SOMs), nitrogen (N), phosphorus (P), and potassium (K) are the most important nutrients for crop production.^[94,95] In agriculture engineering, N, P, and K fertilizers are applied to improve the production of crops. However, excessive anthropogenic nutrient inputs have significant side effects economically and environmentally.^[96] As shown in Figure 5a, only a small amount of fertilizers (e.g., N

and P) is consumed by crops and much of them is lost due to leaching, volatilization, and erosion. To adapt nutrient-deprived environments of plants, efficient and accurate detection of nutrient compounds in soil is essential for developing precision agriculture and the sustainability of the environment.^[94,97–101]

The NIR reflectance-based sensors have been utilized to measure the spatial variation of both surface and subsurface soil nitrogen.^[102–104] Optimal wavelengths for predicting the SOM content can be identified by studying the spectral reflectance of soil samples in the IR and visible wavelength regions.^[105,106] Recently, online measurements of the total nitrogen were reported to predict soil nitrogen using NIR spectrophotometry technology.^[47,107,108] Nitrogen in soil that is available for plants exists in an inorganic form, i.e., nitrate (NO_3^-) and ammonium (NH_4^+), and the measurements of the ion concentrations can be effectively utilized to predict the nitrogen content in soil.^[109–111] For example, Garland et al. used laser-induced graphene (LIG) as electrodes for electrochemical ion-selective sensing of plant available nitrogen (i.e., NH_4^+ and NO_3^-) in soil samples (Figure 5b,c).^[112] The LIG electrodes were functionalized with distinct ionophores specific to NH_4^+ (nonactin) or NO_3^- (tridecylmethylammonium nitrate) within poly(vinyl chloride)-based membranes to create distinct solid contact ion-selective electrodes (SC-ISEs) for NH_4^+ and NO_3^- ion sensing, respectively. The LIG SC-ISEs demonstrated detection limits of $28.2 \pm 25.0 \times 10^{-6} \text{ M}$ (NH_4^+) and $20.6 \pm 14.8 \times 10^{-6} \text{ M}$ (NO_3^-), and linear sensing ranges of $10^{-5}–10^{-1} \text{ M}$ for both sensors (Figure 5d,e).

Artigas et al. reported a probe that incorporated three nitrate-selective electrochemical sensors at three different depths and equipped a copper plate reference electrode.^[113] Since the inorganic nitrogen was in ionic state, the ISE and ISFET could be utilized for nitrate and ammonia detection. Ygodina et al. developed an air-gap sensor using the nitrate-ISE and a soil pH electrode structure.^[114] By integrating the ISE with an on-the-go pH mapping design, Adamchuk et al. performed a simulated in-field soil nitrate measurement.^[115] Ali et al. also developed an all-solid-state soil nutrient sensor to measure the nitrate in soil using poly(3-octyl-thiophene)-molybdenum disulfide (MoS_2) nanocomposite as an ion-electron transducing layer. It demonstrated a high sensitivity of 64 mV per decade, a detection range of 1–1500 ppm NO_3^- , and maintenance-free capability over a period of 4 weeks.^[116] A hybrid ISFET/FIA system combining ISFET with flow injection analysis (FIA) was proposed to perform real-time on-the-go soil nutrient sensing.^[117,118] Gieling et al. employed ISFET and ISE to predict liquid fertilizing agents in a horticulture greenhouse.^[119] Their system was able to provide reliable nitrate information for a 1 week period.

Yokota et al. developed an optical sensor based on the photometric detection of the soil nutrients (ammonia nitrogen, nitrate nitrogen, available phosphorus, available iron, exchangeable manganese, and exchangeable calcium). In this optical sensor, the wavelength of light-emitting diode was chosen to fit the absorption band of chemical reagents whose color was developed by reaction with soil nutrients.^[120] Patkar et al. reported an MEMS-based lab-on-chip system with ISE embedded to measure soil nutrients.^[99] The silicon nitride microcantilever could provide nitrate measurement at the sensitivity of pM level when methyltridodecylammonium nitrate and nitrate ionophore VI in the polymer matrix was chosen to

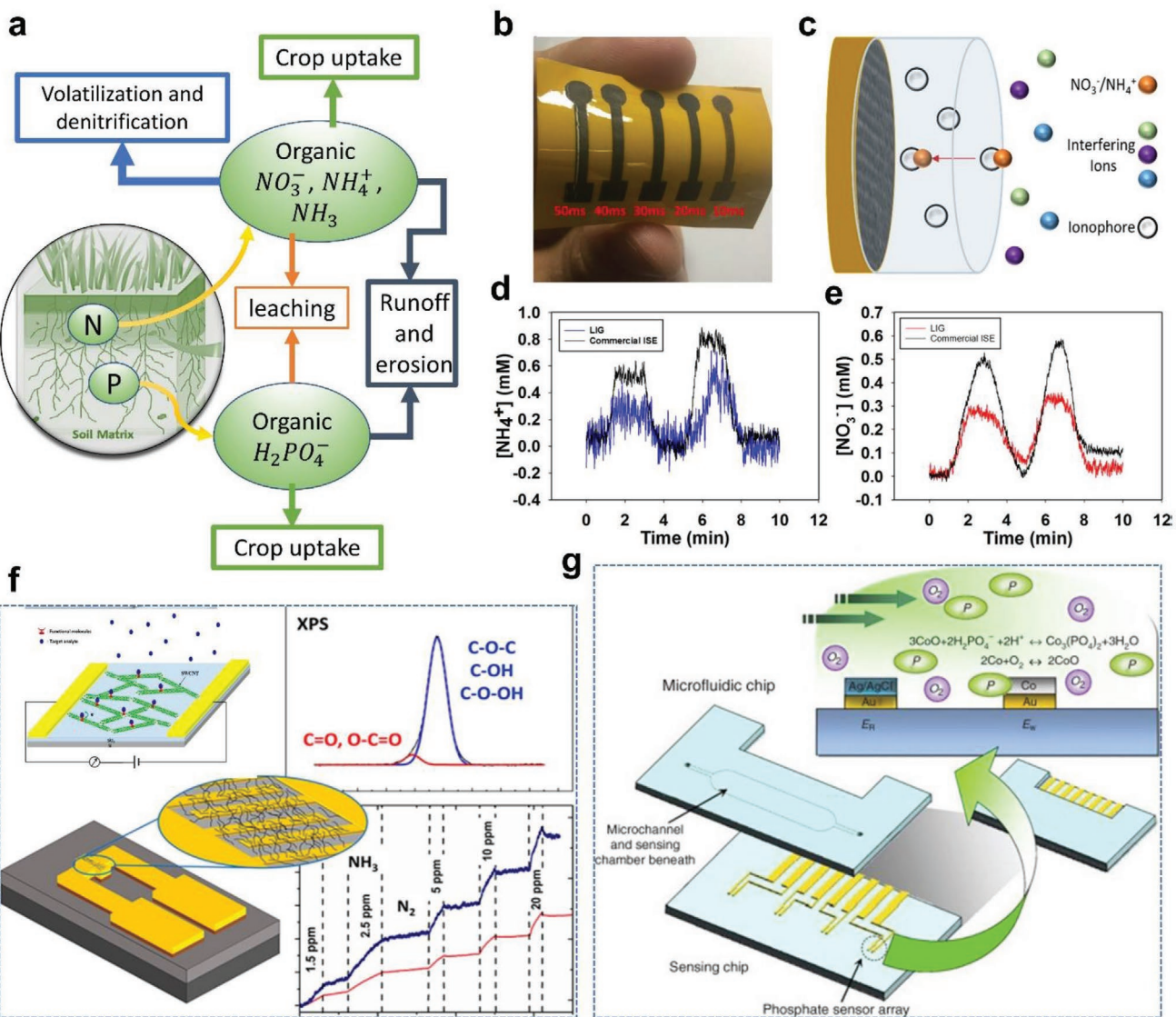


Figure 5. Soil nutrient sensors. a) Schematic illustration of the distribution of organic nitrogen and phosphorus in a soil system. b) Photograph of laser-induced graphene (LIG) solid-contact ion-selective electrodes (SC-ISEs) on a single polyimide swatch. c) Schematic illustration of the SC-ISE ion sensing. d) Measured real time plots of NH_4^+ and e) NO_3^- ions during soil column flush experiments using LIG SC-ISEs compared to commercial ion probes. f) SWCNT-based chemiresistive sensor. The resistance of the SWCNT will be increased with the increase of NH_3 and N_2 concentration. g) A disposable on-chip microsensor with planar cobalt (Co) microelectrodes and Ag/AgCl reference on polymer substrate for phosphate detection in soil extracts. Integrated the microchannel on top of the microfabricated planar cobalt microelectrodes can enhance the throughput by utilizing the advantage of microfluidics. b-e) Reproduced with permission.^[112] Copyright 2018, American Chemical Society. f) Reproduced with permission.^[124] Copyright 2018, American Chemical Society. g) Reproduced with permission.^[136] Copyright 2007, Elsevier.

fabricate the ISEs. Another approach to record nitrogen content variation in soil is to measure the ammonia gas (NH_3) generated through a denitrification process. Optical sensors,^[121] and single-walled carbon nanotube (SWCNT)-based chemiresistive sensors (Figure 5f)^[122–124] have been widely used because of their high sensitivity at ppb level. Instead of directly measuring the nitrogen content in soil, sensing and signal transduction networks were also used to indirectly detect nutrient deprivation in soil through monitoring the plant responses and growth, such as the chlorophyll meter measurement and the normalized difference vegetation index (NDVI) recording.^[94,125–130] For instance, reactive oxygen spe-

cies will rapidly increase after mineral nutrient deprivation. Thus, analyzing the metabolic and morphological responses of plants can sense the nitrogen variation due to the addition of nitrate.^[101]

Similar to the soil nitrogen content sensing, a phosphorus (P) sensing system can utilize UV, visible, or NIR to achieve a noncontact, cost-effective, time-saving, and less laborious measurement of phosphorus concentration in soil.^[98,131,132] VIS or NIR spectroscopy has been demonstrated to measure the P concentration in the soil samples and the in situ soil test.^[133] For example, Jung et al. proposed an NIR sensor with cobalt electrochemical sensing data and developed a data fusion method

to determine phosphorus concentration.^[134] Lemos et al. developed a selective chemical sensor via a phosphorus-selective PVC probe to monitor soil nutrients, establishing a rational process for controlling the use of fertilizers in crops.^[135] Zou et al. reported a disposable on-chip microsensor (Figure 5g) with planar cobalt (Co) microelectrodes and Ag/AgCl reference electrode on a polymer substrate for phosphate detection in soil extracts.^[136] Their microfabricated planar Co microelectrodes showed phosphate-selective potential response over a range from 10^{-5} to 10^{-2} M in acidic medium (pH 5.0) for both inorganic (KH_2PO_4) and organic (adenosine 5'-triphosphate (ATP)) phosphate compounds in soil, exhibiting higher selectivity, higher sensitivity, and better stability than a conventional bulk Co-wire electrode. Although the lifetime of the device was limited to ≈ 30 min only, the proposed phosphate sensor yielded a few advantages such as ease of use, cost effectiveness, reduced analyst consumption, and ease of integrating into disposable lab-on-a-chip devices. Yokota et al. also developed a compact optical sensor that was based on the photometric detection of soil nutrients to detect the phosphorus (P_2O_5), achieving a 1–2 mg/100 g sensitivity.^[120] Lee et al. developed a portable field Raman sensor capable of fast detection and low-cost measurement.^[137,138] The Raman sensor had a laser source at 785 nm with a typical full-width at half-maximum of 0.2 nm and a laser probe assembly with a 1 m optical fiber. This Raman probe can be utilized to obtain a significant P absorption band in soils and to determine P concentration with a sensitivity of 151 mg kg⁻¹. Integrated with nitrogen sensing, NDVI and gene transcriptions can be used to predict the phosphorus status.^[94,131] In addition, integrated lab-on-chip phosphorus analyzers that were developed for water phosphorus monitoring can be applied for soils with high water content.^[139,140]

2.5. Soil Insect/Pest Sensors

Plant diseases and pests may cause significant reduction in both quality and quantity of agricultural products. They could directly damage plant roots and bulbs or first develop and grow in the soil and then become above-ground phytophagous or plant-eating bugs. The major soil pests that induce agriculture loss are beetles, moths, butterflies, flies, and others of equal importance.^[141,142] A few promising methods have been proposed to detect soil pests, including optoelectronic sensors, acoustic sensors, impedance sensors, and nanostructured bio-sensors.^[143,144] For instance, Potamitis et al. proposed a bimodal optoelectronic sensor for automatically monitoring insects (Figure 6a,b).^[145] The bimodal sensor (i.e., electronic e-trap), consisting of Fresnel lenses and associated stereo-recording device, can record the wingbeat events of an insect in flight as backscattered and extinction light. By examining the spectral content of the wingbeats of fruit flies (Figure 6c), it was able to estimate the pest population from the field straight to a human-controlled agency in real-time.

Acoustic sensors can provide nondestructive, remote, and automated detection and monitoring of cryptic insects. The efficacy of the sensors typically depends on multiple factors, including sensor type, frequency range, substrate structure, assessment duration, and the size and behavior of insects.^[146]

The first acoustic insect sensor was based on carbon button microphones.^[147,148] Then dynamic condenser or capacitive microphones were also developed for such purposes, archiving a gain of 60–120 dB and nearly a constant response in the frequency range of ≈ 0 –20 kHz.^[149] Vibration sensors (e.g., accelerometers and piezoelectric disks) are more suitable for signals generated in or under soil.^[150] The sensor–substrate interface can strongly affect the sensitivity and reliability of vibration measurement. Mankin et al. reported an accelerometer sensor system to detect soil insects of 20–30 cm length with an $\approx 100\%$ reliability.^[151] Shuman et al. and Hagstrum et al. developed an automated method using acoustical sensors made of piezoelectric disks to detect insects in stored grain,^[152,153] achieving a 92% accuracy in grading “clean” grain and a 64% accuracy in grading “infested” grain.

Ultrasonic sensors are particularly effective for detecting wood-boring pests because of the negligible background noise at the frequencies of >20 kHz. Using piezoelectric crystals with a resonance frequency of 40 kHz, Mankin and Fisher developed an ultrasonic signal detection system to detect *otiorhynchus sulcatus* larval infestations in nursery containers.^[146,154] The microphones and piezoelectric disks were directly inserted into the soil, while the accelerometers and ultrasonic sensors were attached to a metal waveguide inserted into the soil. One major challenge of using acoustic devices is to distinguish the sounds produced by target species from other sounds. With the rapid progress in reliability, ease of use, and reduced costs, acoustic sensors are expected to have considerable potential in cryptic insect detection and monitoring. Recently, Görres and Chesmore developed an acoustic data analysis method based on the stridulations of larvae for noninvasive species-specific pest monitoring.^[155] The proposed fractal dimension-based data analysis method could automatically detect audio sections with stridulations and provide a semiquantitative estimate of stridulation activity (Figure 6d,e).

Luong et al. developed an impedance sensor—ECIS (electric cell-substrate impedance sensing) to monitor the attachment, motility, spreading, and mortality of adherent insect cells.^[156] The impedance sensor had eight gold electrodes deposited at the bottom of tissue culture wells and immersed in culture medium while the cells were grown on top of those electrodes. The impedance of the device increased upon the attachment and spreading of insect cells on top of the gold electrodes. Airborne remote sensing is flexible and versatile and offers a low-cost alternative for sustainable soil pests management strategy. This kind of sensing depends on the required spatial resolution, high-resolution images, and algorithms for image analysis. For instance, Lan et al.^[157] and Lehmann et al.^[158] reported airborne hyperspectral remote sensing systems by integrating a camera, radio frequency identification, NIR, and color IR or X-ray-based image sensors with an unmanned aerial system or telemetric system. To increase the spatial resolution of insect detection, wireless sensor networks (WSNs), consisting of widely distributed sensing nodes, data communication protocol, and data processing algorithms, have also been developed to predict the insect infestation using multisensory signals.^[159,160] The role of the WSNs in agricultural disease and insect pest control includes the information collection of disease and insect pests and the data processing and analysis

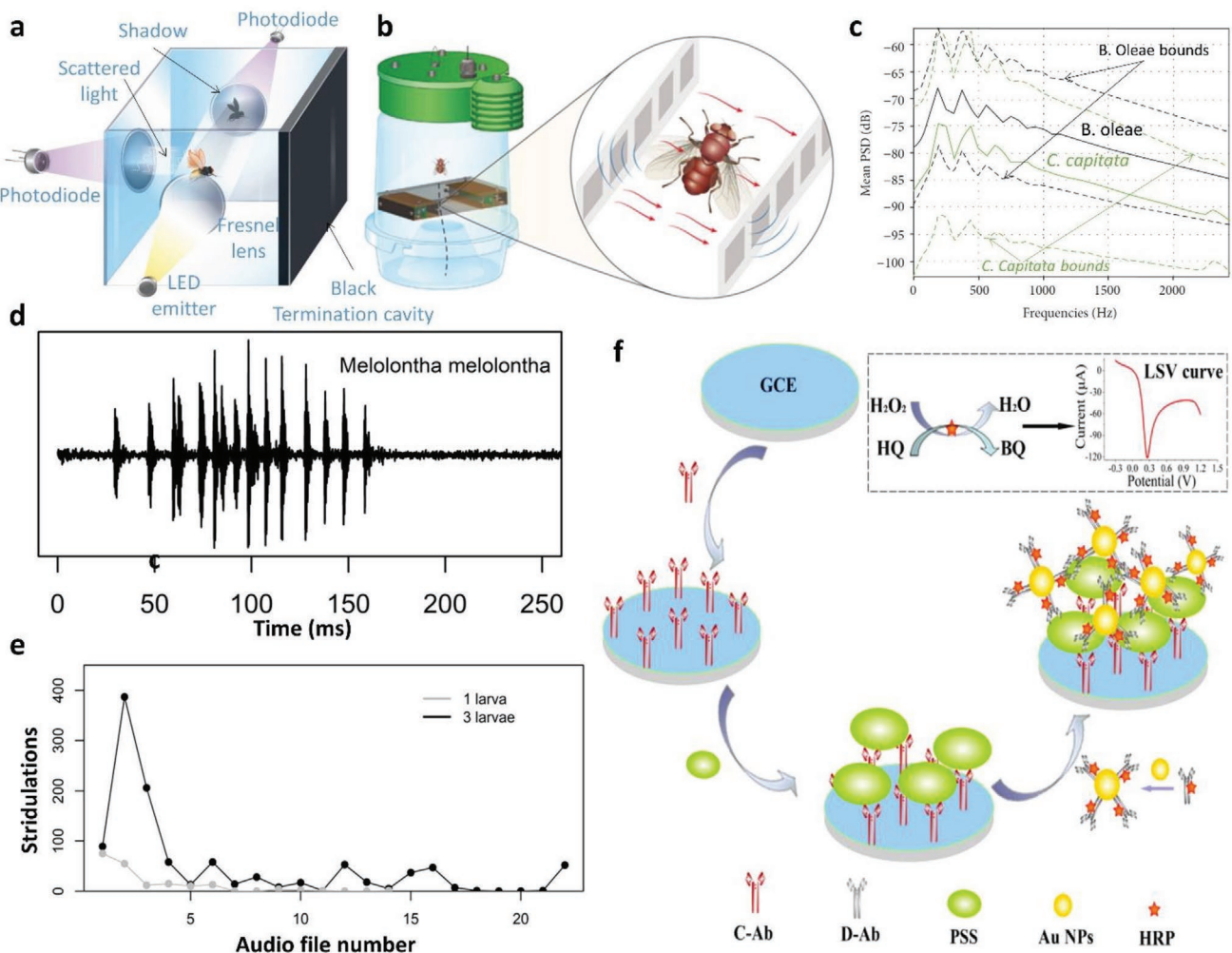


Figure 6. Soil insect sensors. a,b) Schematic illustration of the design and working mechanism of a bimodal optical sensor (electronic e-trap) consisting of Fresnel lenses and associated stereo-recording ability to record the wingbeat spectrum profile. c) Mean \pm SD power spectral densities of scattered light of the wingbeat of *B. oleae* versus *C. capitata*. d) Acoustic patterns produced by stridulation of larvae of *Melolontha hippocastani*. e) Stridulations manually counted in continuous audio recordings of third instar *Melolontha hippocastani* activities in laboratory soil incubations with 1 and 3 larvae, respectively. Each audio file was 50 min long. For the incubation with 1 larva, only 14 audio files were sequentially recorded. f) Schematic illustration of gold-nanoparticles-amplified electrochemical immunoassay for *Pantoea stewartii* ssp. *stewartii* (PSS) detection. a,b) Reproduced and c) Adapted under the terms of the CC-BY Creative Commons Attribution 4.0 International license (<https://creativecommons.org/licenses/by/4.0/>).^[145] Copyright 2018, The Authors, published by Hindawi. d,e) Reproduced under the terms of the CC-BY Creative Commons Attribution 4.0 International license (<https://creativecommons.org/licenses/by/4.0/>).^[155] Copyright 2019, The Authors, published by Springer Nature. f) Reproduced with permission.^[165] Copyright 2014, American Chemical Society.

for guiding the site-specific and time-specific treatments. More details in this aspect will be discussed in Section 4.

The presence of moisture at the soil-air interface or in the top layer of soil is proved to be a hotbed for the development of plant pathogens which may cause severe plant disease and threaten food safety. Compared to nematodes and insects, pathogens can be much smaller in the submicron scale, resulting in the detection failure of the traditional probes.^[161,162] Nano-technology-based biosensors can deliver fast, accurate, cost-effective, and in-field analysis of plant pathogens.^[163] Applying synthesized biocompatible nanosized CdSe quantum dots (QDs) with the DNA probe, Bakhori et al. exploited the fluorescence resonance energy transfer (FRET) technology to detect the synthetic oligonucleotide of DNA for *Ganoderma boninense*,

an oil palm pathogen.^[164] The FRET approach with QDs could determine the hybridization process, demonstrating a high sensitivity and a low detection limit of 3.55×10^{-9} M. Due to a high surface-to-volume ratio, gold nanoparticles (Au-NPs) have been employed for pathogen detection with low detection limits and high specificity. As shown in Figure 6f, Zhao et al. reported a dual amplified electrochemical sandwich enzyme-linked immunoassay (ELISA) to tag the Au-NPs with the Horseradish peroxidase (HRP) antibodies to detect *Pantoea stewartii* ssp. *stewartii* (PSS) plant bacterial pathogen. A linear sweep voltammetry curve between current response and PSS concentration was established with a limit of detection (LOD) of 7.8×10^3 cfu mL⁻¹ in ≈ 30 min.^[165] Siddiquee et al.^[166] modified gold electrode with a ZnO-NPs/Chitosan nanocomposite membrane to develop an

electrochemical DNA biosensor for the identification of a soil-borne fungi *Trichoderma harzianum*, reporting a highest sensitivity, a LOD of 1.0×10^{-19} mol L⁻¹ among all nanostructure biosensors for plant pathogen detection.

2.6. Soil Pollutant Sensors

A number of undesirable heavy metal accumulation, industrial waste, pesticides, herbicides, and hydrocarbon pollution inappropriately entering soil will generate soil pollution or contamination,^[167,168] which will pose severe risks to human health and ecosystem. Currently the concerns to soil pollutants in agriculture are mostly the heavy metals, herbicides, and hydrocarbons.^[169] Extensive use of herbicides and pesticides poses far-reaching consequences due to the significant runoff and leaching of these compounds through soil resulting in water and food contamination.^[170] In this regard, Prasad et al. employed a differential pulse anodic stripping voltammetry method to fabricate a double-template molecularly imprinted polymer nanofilm-modified pencil graphite electrode, which can simultaneously analyze phosphorus-containing amino acid-type herbicides such as glyphosate (GLY) and glufosinate (GLU) in soil.^[171] They immobilized Au nanoparticles and directly grew a nanostructured polymer film on the substrate decorated with monomeric molecules. The modified sensor exhibited a wide linear range from 3.98 to 176.23 ng nL⁻¹ and 0.54 to 3.96 ng nL⁻¹ with detection limits as low as 0.35 and 0.19 ng mL⁻¹ for glyphosate and glufosinate, respectively. Recently, Dong et al. developed a methyl parathion sensor using multiwalled carbon nanotubes–CeO₂–Au nanocomposite (MWCNTs–CeO₂–Au). The sensors reached an ultralow detection limit of 3.02×10^{-11} M for methyl parathion.^[172]

Compared with electrochemical methods, biosensors or immunosensors are more widely utilized in herbicide detection. For example, Tang et al. developed an electrochemical immunosensor using a disposable and conductive chitosan/gold nanoparticle composite membrane and reached a detection limit of 5 ng mL⁻¹ for picloram.^[173] They encapsulated the self-synthesized picloram antibody in the immune membrane to form an immunoconjugate by a competitive immunoreaction, followed by immobilizing the HRP-labeled secondary antibody. Baskeyfield et al. reported a membrane-based immunosensor using a heterogenous competitive ELISA to detect another common herbicide isoproturon, achieving a detection limit of 0.84 ng mL⁻¹.^[174] Carbon working electrodes (WEs) and silver–silver chloride pseudo-reference electrodes (REs) were screen-printed to incorporate a membrane contacting with the WE to facilitate signal transduction. After applying the HRP-labeled polyclonal antibody, an immobilized isoproturon-ovalbumin conjugate-contained membrane was then laminated on top of the WE. Similar immunosensor systems were also reported to detect atrazine and parathion.^[175,176]

Due to the increased soil contamination problems related to heavy metals, the needs for measuring heavy metals in soils have explosively grown in the past few years. By designing an acrylic mold with an applied parallel capacitor method, Lee et al. studied the imaginary part of the dielectric constant of contaminated soil samples in the frequency range from 75 kHz

to 12 MHz.^[177] Hung et al. developed a selective colorimetric method to detect aqueous mercuric, silver, and Pb ions using label-free gold nanoparticles (AuNPs) and selected alkanethiols induced the degree of AuNPs aggregation in the presence of target cation.^[178] As shown in Figure 7a, for the detection of individual or multiple heavy metals, different research groups using electrochemical electrodes have reported the sensitivity of ug L⁻¹ level with both amperometric and voltammetric methods.^[179–181] The electrochemical sensors for heavy metal detection can be improved to get better sensitivity or selectivity by modifying the electrode surface with nanoparticle coatings or ion-selective membrane coatings.^[182–190] Real-time on-site sensing of heavy metal is always a challenging task due to the requirement of the electrolytes for electrochemical reactions. Recently, microfluidic paper-based analytical devices (μ PADs) for electrochemical sensing was developed (Figure 7b) using passive capillary-force to transport sampled fluid through patterned paper channels into distinct detection zones that contain the reagents for specific electrochemical assay.^[191–193] The μ PAD allowed for shorter collection time and combined sampling and analysis in a single device, exhibiting an extremely high sensitivity of up to 0.12 μ g (Cr) and 0.25 ng (Cd and Pb).^[193]

Bioavailable or bioassays sensors are another common technology for detecting soil heavy metals.^[98,168,194,195] Based on the sensing techniques or the transducer components, bioavailability sensors can be categorized into three major types: electrochemical microbial biosensors, conductometric (impedance) sensors, and optical microbial biosensors. Wang et al. reported a P-benzoquinone-mediated amperometric biosensor based on real-time monitoring of inhibition effect on metabolism for detecting multiple heavy metal ions with a sensitivity of \approx mg L⁻¹.^[196] Conductometric enzyme-based biosensors having excellent sensitivity performance were also developed based on the variation of conductivity induced by pollutants.^[197–199] For example, Chouteau et al. utilized the algae enzymatic reaction to detect local conductivity variations, achieving a LOD of 1 ppb for cadmium (II).^[198] Microbial whole-cell sensors have been widely used to assess the bioavailability and the risk of toxic elements, but their environmental use, i.e., soil heavy metal pollution monitoring, is still limited due to the presence of other interfering pollutants and nonspecific binding in cells. For example, Hou et al. reported bioluminescent detection of heavy metal in polluted soil by combining an *E. coli* sensor set with binary regression models for the specific detection of bioavailable cadmium (Cd), lead (Pb), and arsenic (As).^[200] Ivask et al. developed two recombinant bacterial sensors (one for Cd and the other for Pb and Cd) to determine the bioavailability of heavy metals in soil–water suspensions and particle-free extract.^[201] Wei et al. presented a luminescent reporter gene system that could detect a concentration of Hg at 200×10^{-9} M by fusing the mercury-inducible promoter, PmerT, and its regulatory gene, merR, with a promoterless reporter gene EGFP.^[202] Optical biosensors based on green fluorescent *E. coli* for evaluating the toxicity of soil heavy metals were also reported by several groups.^[203–205] For example, Hossain and Brennan proposed a solid-phase bioactive lab-on-paper sensor (Figure 7c) for rapid, selective, and sensitive detection of heavy metals in soil. Their sensor was inkjet printed with sol-gel entrapped reagents to allow the colorimetric visualization of the enzymatic activity

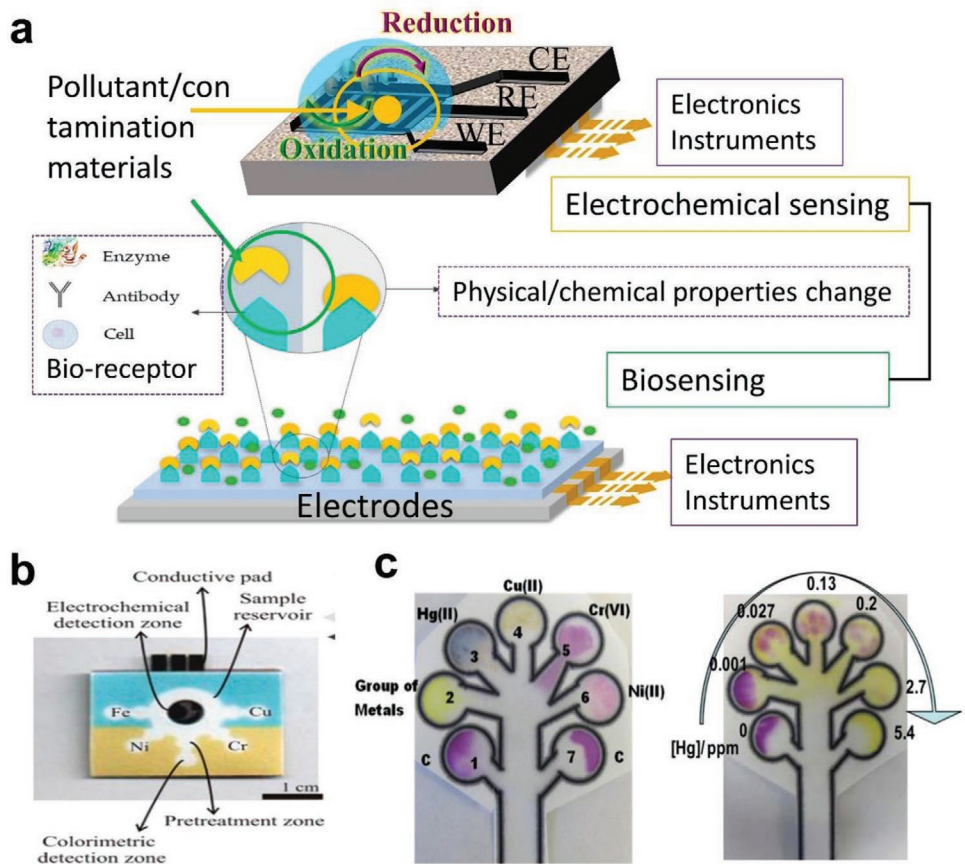


Figure 7. Soil pollutant/contamination sensors. a) Schematic diagram shows the structure of electrochemical sensing and biosensing groups. b) A microfluidic paper-based analytical device (μ PAD) used the passive capillary-driven flow of aqueous through patterned paper channels to transport sampled fluid into distinct detection zones that contain the reagents for specific electrochemical assay. c) A solid-phase bioactive lab-on-paper sensor inkjet printed with sol-gel entrapped reagents. The colorimetric visualization of the enzymatic activity of β -galactosidase works as a detector of toxic heavy metal ions. The image on the right is the colorimetric result of different Hg concentration. a,b) Reproduced with permission.^[193] Copyright 2014, American Chemical Society. c) Reproduced with permission.^[206] Copyright 2011, American Chemical Society.

of β -galactosidase (B-GAL).^[206] The β -galactosidase-based colorimetric paper sensor could record multiple heavy metals simultaneously and exhibited an excellent sensitivity of 0.001 ppm LOD for Hg.

3. Fabrication Approaches for Soil Sensors

With the development of advanced manufacturing methods, in particular the micro-/nanofabrication technology, precise control of sensors can reach micro or even submicron accuracy, which not only enhances the sensor performance greatly but also reduces the sensor size to meet the spatiotemporal resolution requirement.^[207,208] Although detailed procedures for manufacturing may vary significantly for different soil sensors, considering the similar protocols and equipment used in the process, the fabrication approaches for soil sensors can be summarized into two major categories: lithography-based fabrications and printing methods (or additive manufacturing methods).

Lithography-based fabrication processes (Figure 8), either bottom-up or top-down, typically require restricted

clean-room environments and expensive facilities. As shown in Figure 8a, the lift-off process is a typical bottom-up process which adds sensing materials onto the substrate step by step; while the etching process in Figure 8b is a top-down process which removes the unwanted pattern away from the substrate. The key step of this microfabrication process is the pattern generation step, known as a lithography process. By utilizing optical sensitive material, photoresist, and patterned mask, with specific UV light exposure and a following development process, the pattern that was designed in the mask can be transferred into a photoresist layer, which serve as the pattern define layer for the following lift-off or etching process. For example, the graphene QD soil moisture sensor developed by Kalita et al. utilized a lift-off process to form the IDE electrodes,^[44] while the on-chip piezoresistive soil temperature sensor developed by Jackson et al. utilized an etching process to fabricate the microcantilevers.^[66]

Although lithography-based fabrication in cleanrooms can push the sensor feature size down to nanometer level with excellent repeatability and reliability, the requirement of using expensive fabrication facilities could put a heavy

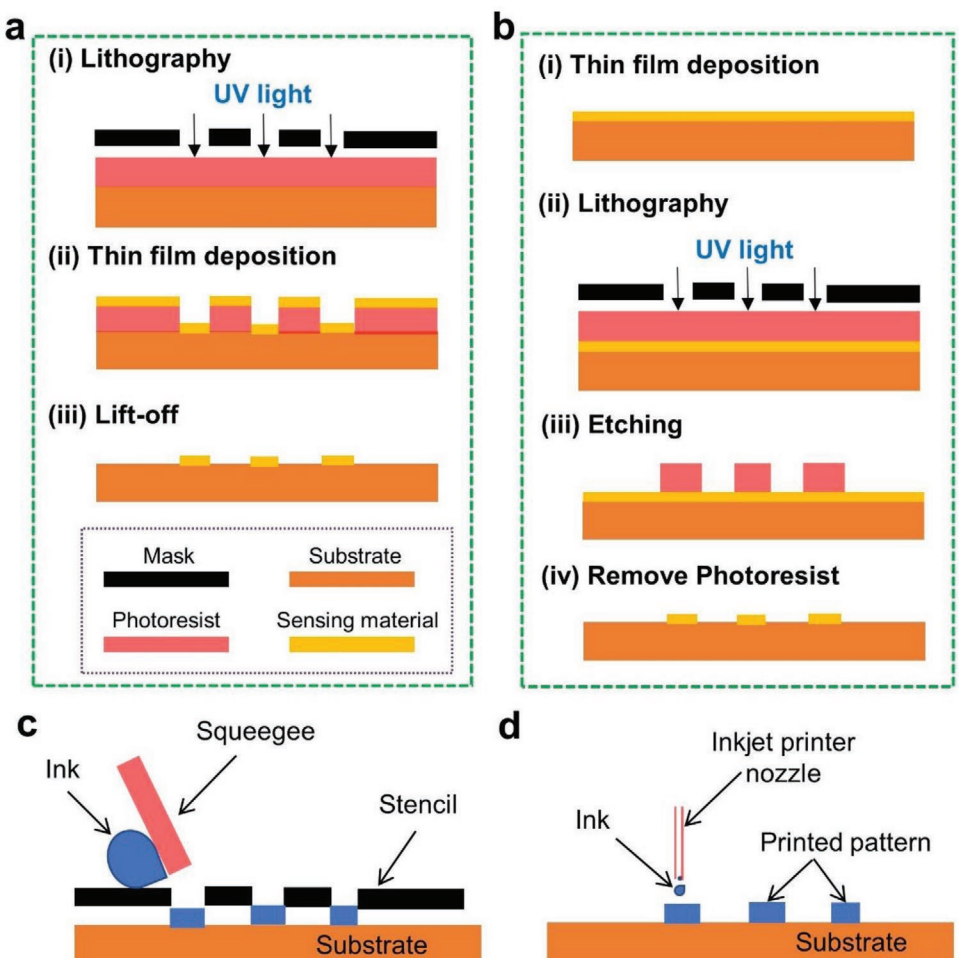


Figure 8. The fabrication approaches for soil sensors. a) Bottom-up fabrication process that typically consists of i) lithography, ii) thin-film deposition, and iii) lift-off process. b) Top-down fabrication process which typically consists of i) thin-film deposition, ii) lithography, iii) etching, and iv) surface cleaning. c) Screen printing method. d) Inkjet printing method.

burden on the cost of final sensors. In contrast, printing methods, such as screen-printing method (Figure 8c) and inkjet printing method (Figure 8d), have drawn increasing attention due to the merits of ease of use, low requirements for manufacturing environments, and saving of materials. For example, the potentiometric Ag/AgCl pH sensor developed by Cranny et al. utilized a screen-printed approach.^[86] With the help of a stencil as the mask in the patterning process, screen printing can greatly increase the fabrication efficiency and provide a thicker film for enhanced conductivity of the electrodes. However, the resolution of the stencil as well as the ink spreading problem of screen-printing method constraint the feature size of sensors. Compared to screen printing, inkjet printing, using a precisely manufactured nozzle, can directly write desired patterns onto the target substrates with a resolution of tens of microns. For example, Sui et al. utilized a low-temperature inkjet-printing technique to fabricate a silver-based soil temperature sensor with a feature size of several hundreds of microns,^[63] while Oren et al. developed an inkjet-printing-based roll-to-roll approach to fabricate graphene-based strain sensors that had a feature

size of 20 micrometers.^[209] Both fabrication methods can be used for fabricating sensors on rigid substrates (e.g., silicon and glass) or flexible/stretchable substrates (e.g., polydimethylsiloxane (PDMS) and polyimide). For example, Nasar et al.^[210] demonstrated a stretchable strain sensor on a PDMS substrate. As a summary, lithography-based fabrication has excellent advantages regarding the fabrication resolution and yield, while printing methods provide the potential to significantly reduce the manufacturing cost as long as the fabrication limitations can be further overcome.

4. Smart Agriculture System

4.1. Soil Sensor Network

Soil properties are spatially and temporally varying,^[211,212] which bring up the challenge in achieving a high accuracy in landscape monitoring. If relied on remote measurements, some interfering factors can limit the spatial and temporal resolution while the on-the-go sensors are generally labor-intensive

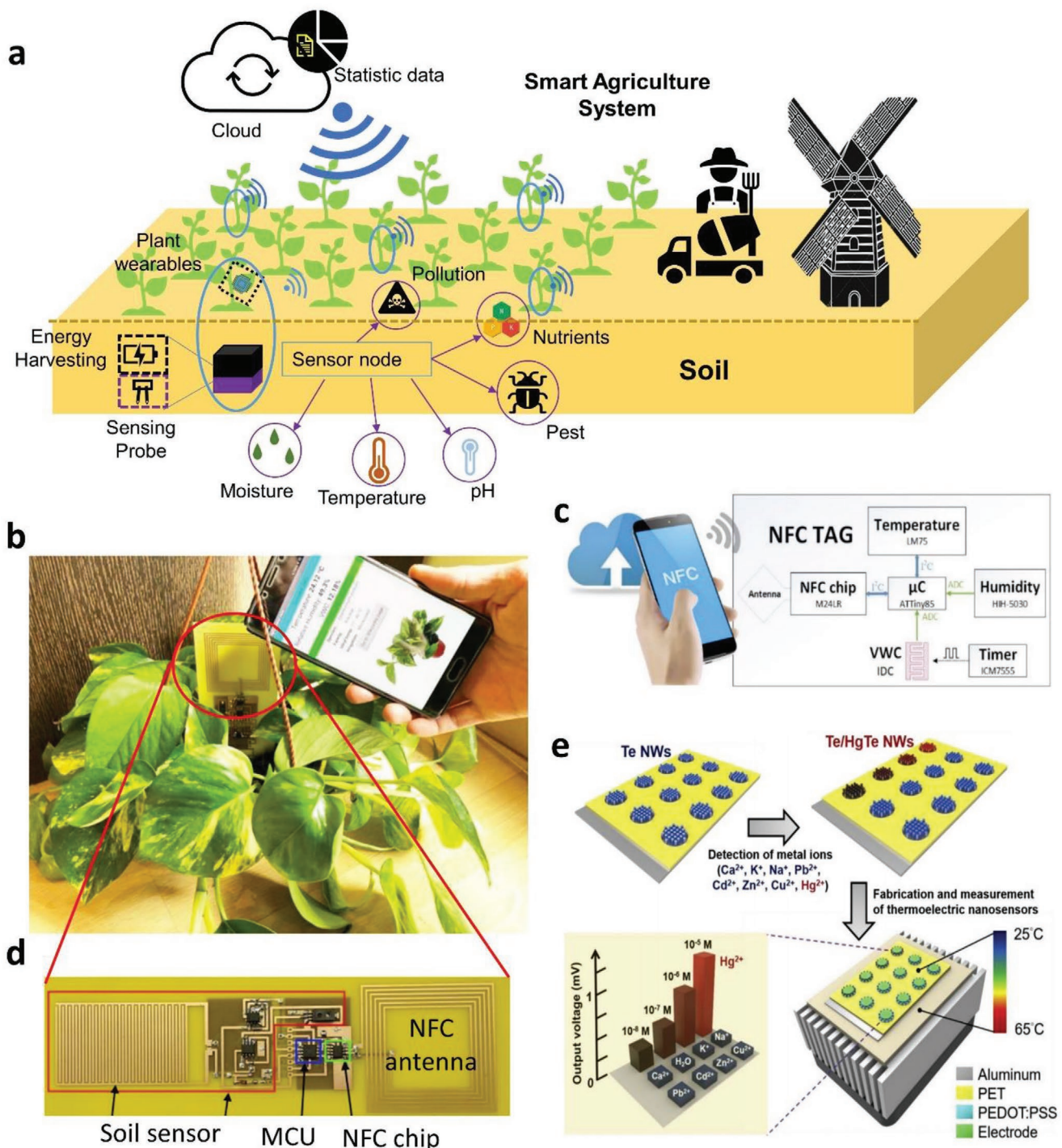


Figure 9. Wireless sensor networks (WSNs) for smart and precision agriculture. a) Schematic diagram of a smart agriculture system. Soil sensing nodes consist of multiple soil sensors, inserted into the soil. The plant wearables are attached on the surface of plants. The deployment density of the sensor nodes and plant wearables can be adjusted based on the spatial resolution and the detection range of the sensors. Wireless communication is used to collect data from all the sensing node and data will be stored in the Cloud. b-d) Plant wearables utilized near field communication (NFC) technology to transmit the data information to a cellphone for wirelessly recording the real-time plant growth. e) Self-powered nanosensor made of tellurium nanowires (TeNWs). The TeNWs acted as a sensing material for mercury ion detection and also a thermoelectric material for energy harvesting. PEDOT:PSS and Ag paste were sequentially coated to form a thermoelectric nanocomposite. b-d) Reproduced with permission.^[225] Copyright 2018, IEEE. e) Reproduced with permission.^[228] Copyright 2019, Elsevier.

and recourse-consuming.^[211] As shown in Figure 9a, the use of a WSN with coarsely distributed sensors, especially in-site

underground soil sensors, provides a feasible solution to improve our capability to regulate the soil environments.^[213,214]

WSN technology can allow real-time soil water content monitoring with a high spatial and temporal resolution for observing hydrological processes in small watersheds. For example, Bongena et al. developed a wireless soil water content network (SoilNet) using a low-cost ZigBee radio network for communication and a hybrid topology connecting both underground sensing devices and aboveground router devices.^[215,216] The SoilNet system consisted of three different components, i.e., the coordinator for storing information and providing a link to other networks, the router acting as a relay station data transmission, and the soil sensors to detect and communicate with their parent nodes (either a coordinator or a router). The impacts of soil depth, soil water content, and soil electrical conductivity on the signal transmission strength of SoilNet were determined by a validated model. In the case of 5 cm depth, sufficient power remained to ensure data communication over longer distances for most soil conditions. The factors controlling the longer travel time reduced the spatial variability of the SoilNet. Vuran and Akyildiz also developed a wireless underground sensor network to study the propagation characteristics and effects of variations in soil moisture. They derived the channel models to perform both theoretical and numerical analysis to prove the feasibility of wireless communication in the underground environment and highlighted several important aspects in this field.^[217] Cardell-Oliver et al. developed a reactive soil moisture sensor network through specific hardware and software design, being reactive to the events such as rain falls and dry periods between rainfalls.^[218] Bayrakdar performed a mathematical simulation with an insect pest detection WSN system, which also revealed the depth variation.^[219] The signal decay with depth variation, the sensor faults, and network redundancy and tolerance were the main challenges that needed to be addressed for an efficient WSN system in precision agriculture.^[220,221]

Developments of low-power, long-duration sensor networks have typically required sufficient energy sources and the regulations for each sensor. Most existing WSNs utilize the rechargeable battery combined with solar energy harvesting as the energy source to achieve continuous operation without the need to replace energy storage.^[213,222,223] However, the ability to harvest solar energy is greatly reduced in environments such as forests due to the shading and frequent dense foliage. Moreover, the efficiency of energy transmission from the aboveground solar energy harvesting devices to the underground sensors as well as the battery performance also pose great risks in the continuous usage of the sensors and the reliability of the WSNs. Toba and Kitagawa developed a wireless moisture sensor on the basis of the backscatter characteristic of the microstrip antenna which worked in the far field without a battery.^[224] With the electromagnetic wave power supply from a transmitter, the backscattered power at the frequencies of 0.954 and 2.45 GHz was measured as an index to soil moisture level. Boada et al. developed a battery-less soil moisture measurement system (Figure 9b-d) based on a near field communication (NFC) device with energy harvesting capability.^[225,226] The soil moisture sensing platform used an NFC-tag to harvest energy from nearby cell phones to power the sensor. The magnetic field generated by a smartphone is stable enough to power up the battery-less NFC-tag for moisture measurement and

data transmission. However, the power level of NFC can only ensure a communication distance of ≈ 3 m which requires the power source, such as smartphones, to be close enough to the sensor, limiting its broader applications.

In comparison, thermoelectrically energy harvesting methodologies that utilize the surrounding temperature difference fit the soil WSN application much better.^[227] As shown in Figure 9e, Tsao et al. developed a self-powered mercury ion nanosensor based on the thermoelectric effect and chemical transformation mechanism.^[228] In their design, tellurium nanowires (TeNWs, Seebeck coefficient $564 \mu\text{V K}^{-1}$) acted both as the core material to generate electric output by temperature difference in the surrounding environment and as the sensing material for mercury ions. Moreover, through the specific reaction between Hg^{2+} ions and TeNWs, a layer of HgTe nanocrystals with a higher Seebeck coefficient of $1829 \mu\text{V K}^{-1}$ was formed to enhance the thermoelectric efficiency of energy harvesting. Yang et al. developed a polarized poly(vinylidene fluoride) film-based flexible hybrid nanogenerator to harvest thermal and mechanical energies.^[229] They demonstrated a cyclic voltage/current pulse from $-2.5 \text{ V}/-24 \text{ nA}$ to $3.2 \text{ V}/31 \text{ nA}$ by changing the temperature from 295 to 314 K. As the environmental temperature typically changing cyclically with day and night alternation, Kwan et al. developed a bidirectional operation of the thermoelectric energy harvesting device by integrated a switch with the thermoelectric (TE) device to successfully harvest heat energy from both thermoelectric generator effect (TEG) and thermoelectric cooling effect (TEC).^[230] Considering that the temperature difference between the soil underground and the air on top of the earth also varies through time, integration of bidirectional operational energy harvesting systems with the soil sensor will allow us to collect data continuously over a 24 h period per day without break.

With the collected data from sensor nodes and the prediction capability via machine learning technologies, irrigation and fertilization for soils can be implemented in a more efficient manner that matches the needs of plant growth to maximize crop production while reducing the waste. In addition, soil sensor networks are also able to supply accurate information about the soil degradation, environmental conditions, and arable land loss in a region due to anthropological activities and/or climate change, which are critical to decision-making of taking necessary actions and implementing public policies.^[231] Some major challenges for widely deploying large-scale sensor networks include the short life-time, low reliability, and difficult maintenance of soil sensors, the efficiency of wireless data transmission, and the reliable models for plant growth based on efficient machine learning algorithms. Future smart and precision agriculture systems are expected to equip large-scale self-powered sensor networks and be capable of system intelligence to predict the plant growth and optimize the management of agriculture production, achieving a sustainable and productive agriculture system.^[231-234]

4.2. Plant Wearables

Wearable devices, i.e., electronic devices that can be incorporated into clothing or worn on the body like accessories, have

been extensively studied in biomedical applications to continually track biometric information related to health or fitness. The concept of wearable devices has been extended to plants due to their capability to continually track important physiological and pathological parameters *in situ*, also adding the opportunity to integrate remote communication and control. Plant wearables possess great potential to achieve a simple, precise, and continuous monitor of plant health at large scale, when compared to alternative methods such as IR fluorescence-based nanobionics^[235] and Raman spectroscopy,^[236] which require more intensive instruments for off-site analysis. When integrated with soil sensors that collect microclimate information, plant wearables can correlate the effect of microclimate on the growth of plants. This correlation has a great impact on maintaining optimal growth settings, thereby resulting in augmented agriculture outputs with minimal agricultural inputs.

Thin-film plant wearables (TFPWs) are of great interest due to their noninvasive and flexible features, which also integrate compliance with irregular plant tissue surfaces. TFPWs are suitable to monitor environmental parameters such as temperature, humidity, and biotic parameters including water potential, displacement/strain of plant tissue, and volatile organic compounds. For example, Lee et al. developed all-carbon film electronics (i.e., field-effect transistors (FET) sensors) using SWCNTs-graphite that can be integrated with live plants for real-time, wireless sensing of toxic gases with a resolution of ppm concentration (Figure 10a–c).^[237] The flexible sensors demonstrated a superb mechanical flexibility and good adhesion to the nonplanar surfaces of biomaterials, which offers unique potential for wearable electronics and bioimplantable sensors. Tang et al. fabricated a flexible and stretchable sensor by directly writing chitosan-based water ink on plants to record the response of plants to mechanical injuries as well as the methyl parathion and nitrite variation.^[238,239] Resistance variation of the printed sensors arising from the strain change due to mechanical injury (cutting) was found to be able to monitor plant wounding. As shown in Figure 10d, Oren et al. proposed a flexible microscale plant tattoo sensor by patterning and transferring graphene-based nanomaterials onto various types of tape.^[209] This sensor estimated hydraulic conductivity by measuring water transportation time from root to leaves and transpiration level of plants based on changes in the electrical resistance of graphene in different moisture environments. Hydraulic conductivity and transpiration level of plants may be used as an indicator for environmental temperature and drought stress in plants. As an alternative to the monitoring of water content in the proximity of stomata, Koman and co-workers targeted stomata behaviors to monitor plant responses to various abiotic stresses.^[240] They developed a stomatal electro-mechanical pore size sensor, allowing for real-time tracking of the single stomatal opening and closing *in planta* via resistance change of a circuit across a stoma composed of carbon nanotubes. Environmental conditions such as soil water potential, incident light intensity, and diurnal cycle could be detected via monitoring stomatal opening and closing, corresponding to a higher and lower hydraulic resistance, respectively. Kim et al. recently deposited conformal conjugated polymer electrodes, p-doped poly(3,4-propylenedioxothiophene) (PProDOT-Cl), via a vapor printing method directly onto living

plant tissues (Figure 10e), which enabled on demand long-term health monitoring (e.g., tissue damage caused by dehydration and UV exposure) using a bioimpedance spectroscopy, a sensitive analytical technique capable of quantifying cellular water content thus diagnosing many biotic and abiotic stress factors in plants, particularly drought stress.^[241] The new electrode for plant wearable showed excellent adhesion to plant tissues during a period of 130 days and great biocompatibility without attenuating the natural growth pattern and self-sustenance of the plants. An integrated plant wearable with temperature, humidity, and stretchable strain sensors was recently proposed by Nassar et al. (Figure 10f,g). In their design, the temperature and humidity sensors monitored the local levels from the surface of the plant's leaf, while the strain sensors quantitatively monitored plant growth in terms of elongation, correlating plant growth with the surrounding environment. A programmed chip and an ion battery were also employed on-site, enabling continuously monitoring, data storage, and remote communication (Figure 10h).^[210] This self-powered integrated plant wearable showed promising potential in both in-lab research on the interface of plant-microenvironment and in-field long-term monitoring of the environment and plant growth. Indeed, a 3D-printed origami-based PlantCopter design was also implemented for large field microclimate monitoring application.^[210] Subcellular scale sensors enlightening from plant, mainly nanosensors and nanobionics,^[242,243] are not considered plant wearables and will not be discussed here.

Different from adhesive thin-film plant wearables detecting on the surfaces of plants, microneedles have shown their ability to reach vasculature inside the plants with minimal invasion,^[244,245] thus enabling both to detect sap flow rate and to extract sap and analyze its composition and physicochemical properties such as pH and electric conductivity. Baek and co-workers fabricated a microneedle sap flow sensor based on the modified Granier sap flow method to monitor water transportation in tomato plant stem,^[244] which can potentially be used to indicate changes of environmental variables, e.g., solar intensity, humidity, and soil water content. Another metal microneedle-based plant wearable (Figure 10i) with excellent mechanical robustness was developed,^[246] capable of repeated insertion into sorghum tissues without deformation. By measuring the impedance of stalk, root crown, or leaf in reference to soil, the drought conditions and the rehydrating process could be estimated. In a recent study, Jiao et al. reported a microneedle-like integrated plant nitrate detection wearable, including an insertable silicon chip that consists of a nitrate-selective field effect transistor, a temperature sensing unit, and a silver/silver chloride (Ag/AgCl) reference electrode (RE), a readout circuit that collects signals, and an SD card for signal storage.^[247] The plant wearable was demonstrated to continuously detect and quantify nitrate concentration inside the plant under different light patterns, irrigation, and fertigating management.

However, it is worth noting that there are some intrinsic drawbacks in plant wearables discussed above. For example, premade thin-film plant wearables may suffer from mismatching with the irregular and complex plant tissue surfaces when adhered to plants, resulting in lower accuracy and even dysfunction, although the premaking procedure enables fast and large-scale fabrication. The mismatching will dramatically

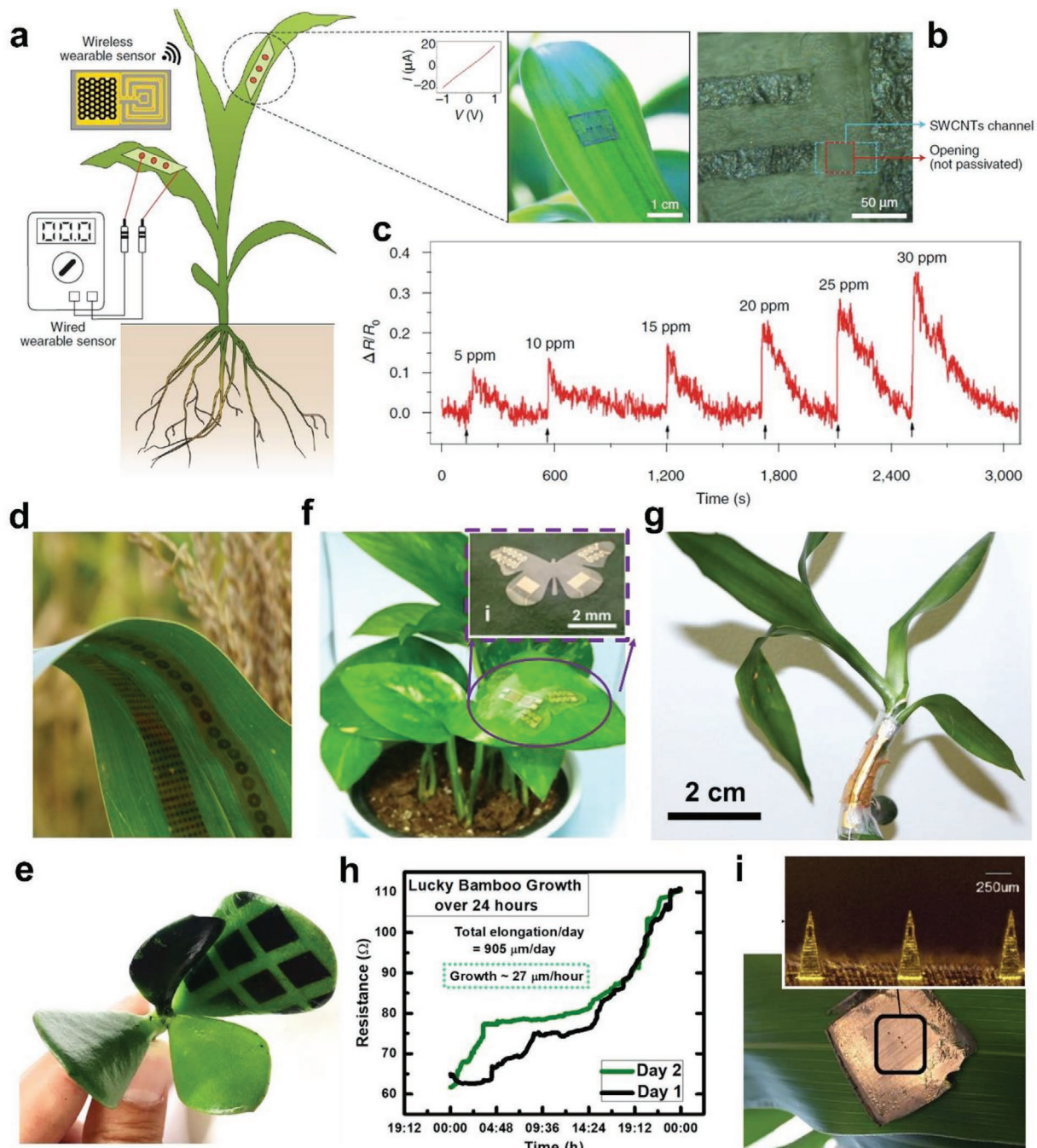


Figure 10. Plant wearables. a) Plants engineered with wireless and wired wearable sensors for chemical sensing on crop leaves. b) A photograph and optical microscopy image and of an SWCNTs FET sensor transferred onto the surface of a live leaf. c) Radio-frequency wireless sensing of a volatile nerve agent simulant DMMP (dimethyl methylphosphonate) with ppm concentration resolution. d) Flexible microscale plant tattoo sensor fabricated by patterning and transferring graphene-based nanomaterials onto flexible tapes. e) Jade plant coated with a PProDOT-Cl electrode pattern achieved using a polyimide tape mask placed on a leaf. f) A compliant plant wearable by integrating ultralight multisensory platform that was placed right on the leaf surface, and a packaged stretchable strain sensor that was placed along the stem and internodes of the plant. g) Digital photographs displaying the seamless integration of the growth strain sensors on the stem of a Lucky Bamboo plant. h) Quantitative and real-time tracking of Lucky Bamboo growth rate continuously for 2 days. i) Prototype of the microneedles as plant wearables to monitor plants experiencing drought and rehydration. a–c) Reproduced with permission.^[237] Copyright 2014, American Chemical Society. d) Reproduced with permission.^[209] Copyright 2017, Wiley-VCH. e) Reproduced with permission.^[241] Copyright 2019, The Authors, published by American Association for the Advancement of Science (AAAS). Reprinted/adapted from ref. [241]. © The Authors, some rights reserved; exclusive licensee American Association for the Advancement of Science. Distributed under a Creative Commons Attribution NonCommercial License 4.0 (CC BY-NC) <https://creativecommons.org/licenses/by-nc/4.0/>. f–h) Reproduced under the terms of the CC-BY Creative Commons Attribution 4.0 International license (<https://creativecommons.org/licenses/by/4.0/>).^[210] Copyright 2018, The Authors, published by Springer Nature. i) Reproduced with permission.^[246] Copyright 2018, The Author, Sandia National Laboratories.

worsen due to remarkable plant tissue size enlargement during growth. This challenge severely hinders long-term monitoring, especially for those fast-growing plants (e.g., most crops and vegetables). One straightforward solution is to develop more flexible plant wearables (e.g., hydrogels), capable of larger deformation and well adhesion to irregular surfaces. Direct fabrication of such wearables on living plant tissues could potentially overcome this mismatching challenge since device components can be deposited along the irregular surfaces,^[235,236] but arises the labor-intensive on-site fabrication procedure under complex environments, particularly in field. This strategy significantly limits the available fabrication conditions because the plants have to survive through the fabrication procedure without harsh conditions. For instance, the vapor temperature must be controlled when deposited on plant tissues in the vapor printing method,^[236] which arises additional requirements to minimize potential damage to plant tissues during fabrication. Thus, printing/writing/deposition of materials on plant tissues under mild conditions is highly desired. Nontoxicity and controlled degradability are favorable properties of wearables especially when used on fruits, vegetables, and crops. Portable devices for direct printing/writing/deposition should be developed for such a strategy, facilitating large-scale in-field operation. Cellular scale plant wearables^[235] detecting localized signals may miss distal signals or signals through other pathways. They also require expertise of microscale fabrication on living tissues.

Microneedle-based plant wearables do not suffer from aforementioned mismatching issue unless they have a microneedle array. The invasive detecting may cause damage to plant, depending on microneedle size as well as the plant size. The detection, particularly long-term detection, may also be blocked by the healing process of plants via isolation of the inserted sensor from sap flow. Thus, wounding responses such as formation of callus should be mitigated or minimized by using biocompatible materials (e.g., pectin, cellulose, hemicellulose, lignin, etc.), decreasing dimensions of the microneedles, and other potential tricks (e.g., biodegradable microneedles loaded with payloads suppressing local wounding responses or accelerate cell healing). In addition, the consistency of performance of all kinds of plant wearables should be investigated in constantly changing weather in-field, such as raining, windy, and even sunny weather, instead of under only neat and well-controlled in-lab conditions. Exposure to rain or sunlight and plant motion due to wind may affect the adhesion of plant wearables and their matching with plants, cause dysfunction, shorten the working life of plant wearables, and produce significant noise signals.

In summary, plant wearables provide a powerful and convenient way to track biometric information *in situ* related to plant growth and health. Continual tracking and remote communication are enabled if storage units and power sources are integrated. Further integration of such plant wearables with sensors detecting environmental conditions such as temperature, light intensity, and relative humidity may provide a powerful tool to investigate the interface of plant-microenvironment, to maintain optimal environments for plant growth, and to boost crop yield with minimal agricultural inputs. There are also certain drawbacks in reported plant wearables

and challenges in their wide applications in agriculture. Special efforts will be needed to overcome the drawbacks discussed above via interdisciplinary combination of materials properties (e.g., strength, compliance, adhesion, biocompatibility, and degradability), fabrication methods (e.g., low cost, large scale, and mild conditions), and particularly morphology and physiology of plants (e.g., signaling in growth and responses to biotic and abiotic stresses, wounding, etc.).

5. Soil Sensors Market

Soil sensors allow constant monitoring of physical and chemical signals in the soil, optimizing crop growth, efficiency of yield and productivity. There is a high demand for the use and development of soil sensors in digital farming, and the market is expected to grow considerably in the next few years.^[248] Soil moisture sensors are the most available type of soil sensors on the market and as such they represent a good example to evaluate the economic and environmental impact of soil sensors. The global market for soil moisture sensors is estimated at US\$147.5 million in 2020 and is projected to reach US\$360.9 million by 2027.^[249] The major drivers for the development of soil sensors are the growing population and need for increased food production, increasingly visible environmental impact of agriculture and changes in climate patterns, need for efficient agricultural practices and water conservation in irrigation systems, and government regulations and initiatives favoring market growth.^[250] Agriculture is the major user of soil moisture sensors, followed by management of residential areas and sport turfs. As the growing trend toward continuous monitoring of crop health and automation, demand for wireless sensor networks in precision farming is expected to increase in the future. However, the challenges posed by diversity and complexity of agricultural decision making, as well as the immature reality of the sensor development and implementation, hold on the high investment cost threshold that impedes the progress of smart/precision agriculture systems. One of the most urgent challenges remains in sensor development enabling noninvasive, low cost, reliable sensors that can be widely distributed to provide real-time soil quality and plant growth monitoring. Along with the sensor development, electronics interfaces that are required to implement the sensors with strict specification requirements, communication of sensor nodes while build up a network with the capability to collect big data at large distances, and system intelligence enable data analysis through machine learning for increasing agricultural productivity and optimized natural resources usage remain under development in laboratory. Enhanced cooperation between research laboratories and the industry to implement the novel sensing technologies with the target to solve the challenges mentioned above will be the key step toward the ultimate goal of smart/precision agriculture.

6. Outlook and Conclusion

We have systematically revisited the major advances in soil sensors as well as their applications in smart and precision

agriculture. We highlighted the six major categories of soil sensors: moisture sensors, temperature sensors, pH sensors, nutrient sensors, pest sensors, and pollutant sensors. Plant wearables that detect the growth and health conditions of crops were also briefly discussed. The working mechanisms, designs, and performances of these sensors were provided, and the pros and cons of each kind of sensor were discussed. Finally, wireless sensor networks and self-power technologies for deployment of smart/intelligent agriculture systems were reviewed. Through the comprehensive review, we believe that the main focuses for future soil sensing will rely on these four aspects: 1) to improve the sensing performance (e.g., sensitivity and specificity) and reliability for key soil parameters, with little interference from background noise; 2) to develop a sufficient low-power consumption WSN with powerful data processing and long-range wireless communication capability; 3) to develop versatile soil sensing platforms that can be distributed in large-scale to collect real-time soil microenvironment data continuously; 4) to develop self-powered or power-independent sensors and sensing platforms that are low-cost, reliable, and maintenance free. Energy harvesting functions may become an essential element for the large-scale deployment of the smart agriculture systems for long-term service. Additionally, versatile plant wearables will be useful tools for precision agriculture development. The functionality, low-cost, compact size, and eco-friendly manufacturing of soil sensors and plant wearables are expected to become major driving forces in advancing sensing systems for smart and precision agriculture. This review provides the key knowledge and better understanding for the new developments of soil sensors in smart and precision agriculture and also sheds light on the research challenges and trends for future study of intelligent agriculture systems.

Acknowledgements

H.Y. and Y.C. contributed equally to this work. This work was partially supported by NSF (ECCS-2024649), USDA-NIFA (Hatch Project 1016788), and Michigan State University. B.M. and Y.C. acknowledge funding from Singapore-MIT Alliance for Research & Technology, National Research Foundation, Prime Minister's Office, Singapore under its Campus for Research Excellence and Technological Enterprise (CREATE) program. X.Z. acknowledges NSF EAGER SITS 1841301.

Conflict of Interest

The authors declare no conflict of interest.

Keywords

plant wearables, precision agriculture, smart agriculture, soil sensors, wireless sensor networks

Received: November 15, 2020

Revised: December 12, 2020

Published online: April 7, 2021

- [1] L. Lipper, P. Thornton, B. M. Campbell, T. Baedeker, A. Braimoh, M. Bwalya, P. Caron, A. Cattaneo, D. Garrity, K. Henry, R. Hottle, L. Jackson, A. Jarvis, F. Kossam, W. Mann, N. McCarthy, A. Meybeck, H. Neufeldt, T. Remington, P. T. Sen, R. Sessa, R. Shula, A. Tibu, E. F. Torquebiau, *Nat. Clim. Change* **2014**, *4*, 1068.
- [2] N. Alexandratos, J. Bruinsma, *World Agriculture towards 2030/2050: The 2012 Revision*, FAO, Rome **2012**.
- [3] R. Gebbers, V. I. Adamchuk, *Science* **2010**, *327*, 828.
- [4] J. V. Stafford, *J. Agric. Eng. Res.* **2000**, *76*, 267.
- [5] N. Zhang, M. Wang, N. Wang, *Comput. Electron. Agric.* **2002**, *36*, 113.
- [6] G. Venter, *Successful Hydroponics: 21st Century Technology for Commercial and Home Applications: A Comprehensive Practical Guide to Scientifically Based Hydroponic Crop Production*, Xlibris Corporation, Bloomington, IN, USA **2010**.
- [7] R. A. Viscarra Rossel, J. Bouma, *Agric. Syst.* **2016**, *148*, 71.
- [8] Soil Sensor Technologies, <https://soilsensor.com/sensors/sensor-technologies/> (accessed: February 2020).
- [9] D. A. Robinson, C. S. Campbell, J. W. Hopmans, B. K. Hornbuckle, S. B. Jones, R. Knight, F. Ogden, J. Selker, O. Wendroth, *Vadose Zone J.* **2008**, *7*, 358.
- [10] S. U. Susha Lekshmi, D. N. Singh, M. Shojaei Baghini, *Meas. J. Int. Meas. Confed.* **2014**, *54*, 92.
- [11] P. Andrade-Sánchez, S. K. Upadhyaya, J. Agüera-Vega, B. M. Jenkins, *Trans. ASAE* **2004**, *47*, 1281.
- [12] H. Eller, A. Denoth, *J. Hydrol.* **1996**, *185*, 137.
- [13] S. Sulaiman, A. Manut, A. R. Nur Firdaus, in *2009 Int. Conf. on Information and Multimedia Technology*, IEEE, Piscataway, NJ, USA **2009**, pp. 513–516, <https://doi.org/10.1109/ICIMT.2009.54>.
- [14] B. G. Williams, D. Hoey, *Aust. J. Soil Res.* **1987**, *25*, 21.
- [15] D. Moghadas, K. Z. Jadoon, M. F. McCabe, *J. Appl. Geophys.* **2019**, *169*, 226.
- [16] D. A. Robinson, H. Abdu, I. Lebron, S. B. Jones, *J. Hydrol.* **2012**, *416–417*, 39.
- [17] B. Kuang, H. S. Mahmood, Z. Quraishi, W. B. Hoogmoed, A. M. Mouazen, E. J. Van Henten, *Advances in Agronomy*, Vol. 114, Elsevier Inc., New York **2012**.
- [18] B. Cardenas-Lailhacar, M. D. Dukes, *Trans. ASABE* **2012**, *55*, 581.
- [19] H. S. Wheater, S. Tuck, R. C. Ferrier, A. Jenkins, F. M. Kleissen, T. A. B. Walker, M. B. Beck, *Hydrol. Processes* **1993**, *7*, 359.
- [20] C. E. Mullins, O. T. Mandiringana, T. R. Nisbet, M. N. Aitken, *J. Soil Sci.* **1986**, *37*, 691.
- [21] R. N. Dean, A. K. Rane, M. E. Baginski, J. Richard, Z. Hartzog, D. J. Elton, *IEEE Trans. Instrum. Meas.* **2012**, *61*, 1105.
- [22] A. M. Thomas, *J. Sci. Instrum.* **1966**, *43*, 21.
- [23] G. C. Topp, J. L. Davis, A. P. Annan, *Water Resour. Res.* **1980**, *16*, 574.
- [24] J. E. Campbell, *Soil Sci. Soc. Am. J.* **1990**, *54*, 332.
- [25] I. White, J. H. Knight, S. J. Zegelin, G. C. Topp, W. R. Whalley, *Eur. J. Soil Sci.* **1994**, *45*, 503.
- [26] M. S. Seyfried, M. D. Murdock, *Soil Sci. Soc. Am. J.* **2004**, *68*, 394.
- [27] M. S. Seyfried, L. E. Grant, K. Humes, *Vadose Zone J.* **2005**, *4*, 1070.
- [28] M. S. Seyfried, L. E. Grant, *Vadose Zone J.* **2007**, *6*, 759.
- [29] S. D. Logsdon, T. R. Green, M. Seyfried, S. R. Evett, J. Bonta, *Soil Sci. Soc. Am. J.* **2010**, *74*, 5.
- [30] J. Miralles-Crespo, M. W. van Iersel, *HortScience* **2011**, *46*, 889.
- [31] B. Will, I. Rolfs, in *2014 IEEE Sensors Applications Symposium (SAS)*, IEEE, Piscataway, NJ, USA **2014**, pp. 233–236, <https://doi.org/10.1109/SAS.2014.6798952>.
- [32] N. Fonseca, R. Freire, G. Fontgalland, B. Arruda, S. Tedjini, in *2018 3rd Int. Symp. on Instrumentation Systems, Circuits and Transducers (INSCIT)*, IEEE, Piscataway, NJ, USA **2018**, <https://doi.org/10.1109/INSCIT.2018.8546707>.

- [33] B. Will, I. Rolfs, in *SENSORS*, 2013, IEEE, Piscataway, NJ, USA **2013**, <https://doi.org/10.1109/ICSENS.2013.6688529>.
- [34] W. Skierucha, A. Wilczek, *Sensors* **2010**, *10*, 3314.
- [35] J. R. Macdonald, *Impedance Spectroscopy: Emphasizing Solid Materials and Systems*, John Wiley & Sons, Inc., New York **1987**.
- [36] A. Robert, *J. Appl. Geophys.* **1998**, *40*, 89.
- [37] G. J. Gaskin, J. D. Miller, *J. Agric. Eng. Res.* **1996**, *63*, 153.
- [38] M. Persson, *Soil Sci. Soc. Am. J.* **1997**, *61*, 997.
- [39] G. Armento, J. M. Baker, C. F. Reece, *Soil Sci. Soc. Am. J.* **2000**, *64*, 1931.
- [40] C. Rusu, A. Krozer, C. Johansson, F. Ahrentorp, T. Pettersson, C. Jonasson, J. Rösevall, D. Ilver, M. Terzaghi, D. Chiatante, A. Montagnoli, *Comput. Electron. Agric.* **2019**, *167*, 105076.
- [41] D. A. DeVries, in *Physics of Plant Environment* (Ed. W. R. van Wijk), North-Holland Publishing Company, Amsterdam, The Netherlands **1963**, pp. 210–235.
- [42] A. J. Clark, *Master's Thesis*, The University of Arizona, Tucson, AZ, USA **1983**, <https://hdl.handle.net/10150/274703>.
- [43] A. Valente, R. Morais, C. Couto, J. H. Correia, *Sens. Actuators, A* **2004**, *115*, 434.
- [44] H. Kalita, V. S. Palaparthy, M. S. Baghini, M. Aslam, *Sens. Actuators, B* **2016**, *233*, 582.
- [45] N. Hiraoka, T. Suda, K. Hirai, K. Tanaka, K. Sako, R. Fukagawa, M. Shimamura, A. Togari, *Jpn. J. Appl. Phys.* **2011**, *50*, 07HC19.
- [46] M. Knadel, A. Thomsen, K. Schelde, M. H. Greve, *Comput. Electron. Agric.* **2015**, *114*, 134.
- [47] J. W. Hummel, K. A. Sudduth, S. E. Hollinger, *Comput. Electron. Agric.* **2001**, *32*, 149.
- [48] A. M. Mouazen, M. R. Maleki, J. De Baerdemaeker, H. Ramon, *Soil Tillage Res.* **2007**, *93*, 13.
- [49] M. Kodaira, S. Shibusawa, *Geoderma* **2013**, *199*, 64.
- [50] Y. Chen, Y. Tian, X. Wang, L. Dong, in *2019 20th Int. Conf. Solid-State Sensors, Actuators and Microsystems & Eurosensors XXXIII (TRANSDUCERS & EUROSENSORS XXXIII)*, IEEE, Piscataway, NJ, USA **2019**, pp. 2025–2028, <https://doi.org/10.1109/TRANSDUCERS.2019.8808562>.
- [51] R. D. Jackson, A. T. Sterling, *Thermal Conductivity and Diffusivity, Methods of Soil Analysis: Part 1 Physical and Mineralogical Methods 5* (Ed: A. Klute), American Society of Agronomy, Inc./Soil Science Society of America, Inc., Madison, WI, USA **1986**, pp. 945–956, Ch. 39.
- [52] F. G. Viets, *Agric. Ecosyst. Environ.* **1990**, *30*, 159.
- [53] M. L. Brusseau, I. L. Pepper, C. Gerba, *Environmental and Pollution Science*, Academic Press, San Diego, CA, USA **2019**.
- [54] F. Stuart Chapin, P. A. Matson, P. M. Vitousek, *Principles of Terrestrial Ecosystem Ecology*, Springer-Verlag, New York **2012**.
- [55] J. M. Kevin, in *Methods of Soil Analysis: Part 4 Physical Methods* (Eds: J. H. Dane, G. C. Topp), Soil Science Society of America, Madison, WI, USA **2002**, pp. 1183–1199, Ch. 39.
- [56] R. P. Benedict, *Fundamentals of Temperature, Pressure, and Flow Measurements*, Wiley, New York **1969**.
- [57] C. Hagart-Alexander, in *Instrumentation Reference Book* (Ed: W. Boyes), Butterworth-Heinemann, Oxford, UK **2010**, p. 269.
- [58] T. D. McGee, *Principles and Methods of Temperature Measurement*, Wiley, New York **1988**.
- [59] R. J. Stephenson, A. M. Moulin, M. E. Welland, J. Burns, M. Sapoff, R. P. Reed, R. Frank, J. Fraden, J. V. Nicholas, F. Pavese, J. Stasiek, T. Madaj, J. Mikielewics, B. Culshaw, in *The Measurement, Instrumentation, and Sensors Handbook* (Ed: J. G. Webster), CRC Press, Cleveland, OH, USA **1999**.
- [60] I. Yolcubal, M. L. Brusseau, J. F. Artiola, P. Wierenga, L. G. Wilson, in *Environmental Monitoring and Characterization* (Eds: J. Artiola, I. L. Pepper, M. L. Brusseau), Elsevier Inc., New York **2003**, pp. 207–239.
- [61] X. Yang, L. Zhao, M. Bruse, Q. Meng, *Build. Environ.* **2013**, *60*, 93.
- [62] H. M. Salem, C. Valero, M. Á. Muñoz, M. G. Rodríguez, L. L. Silva, *Geoderma* **2015**, *237–238*, 60.
- [63] Y. Sui, L. P. Kreider, K. M. Bogie, C. A. Zorman, *IEEE Sens. Lett.* **2019**, *3*, 2500704.
- [64] S. O. Aleksic, N. S. Mitrovic, M. D. Lukovic, S. D. Veljovic-Jovanovic, S. G. Lukovic, M. V. Nikolic, *IEEE Sens. J.* **2018**, *18*, 4414.
- [65] S. B. Wuest, *Soil Sci. Soc. Am. J.* **2013**, *77*, 427.
- [66] T. Jackson, K. Mansfield, M. Saafi, T. Colman, P. Romine, *Meas. J. Int. Meas. Confed.* **2008**, *41*, 381.
- [67] S. S. Nielsen, *Food Analysis*, 4th ed., Springer Science and Business Media, New York **2010**.
- [68] M. I. Khan, K. Mukherjee, R. Shoukat, H. Dong, *Microsyst. Technol.* **2017**, *23*, 4391.
- [69] S. Kumar, R. T. Babankumar, M. Kumar, *Int. J. Adv. Res. Electr. Electron. Instrum. Eng.* **2015**, *4*, 4452.
- [70] Y. Zuo, D. C. Erbach, S. J. Marley, *Trans. ASAE* **1995**, *43*, 1317.
- [71] F. D., *Opt. Lett.* **1997**, *22*, 567.
- [72] Z. Li, J. R. Askim, K. S. Suslick, *Chem. Rev.* **2019**, *119*, 231.
- [73] V. A. Postnikov, *Holographic Sensors for Detection of Components in Water Solutions*, IntechOpen, London, UK **2013**.
- [74] N. Maleki, A. Safavi, F. Sedaghatpour, *Talanta* **2004**, *64*, 830.
- [75] N. F. Sheppard, M. J. Lesho, P. McNally, A. Shaun Francomacaro, *Sens. Actuators, B* **1995**, *28*, 95.
- [76] M. I. Khan, A. M. Khan, A. Nouman, M. I. Azhar, M. K. Saleem, in *2012 Int. Conf. Solid-State and Integrated Circuit (ICSIC 2012)* (Ed: S. Yu), Xian, China **2012**, pp. 18–22.
- [77] N. F. Sheppard, R. C. Tucker, S. Salehi-Had, *Sens. Actuators, B* **1993**, *10*, 73.
- [78] V. S. Palaparthy, M. S. Baghini, D. N. Singh, *Emergency Mater. Res.* **2013**, *2*, 166.
- [79] A. Arshak, E. I. Gill, K. Arshak, O. Korostynska, C. Cunniffe, in *2007 30th Int. Spring Seminar on Electronics Technology (ISSE)*, IEEE, Piscataway, NJ, USA **2007**, pp. 213–218, <https://doi.org/10.1109/ISSE.2007.4432850>.
- [80] M. Simić, L. Manjakkal, K. Zaraska, G. M. Stojanović, R. Dahiya, *IEEE Sens. J.* **2016**, *17*, 248.
- [81] K. Arshak, E. Gill, A. Arshak, O. Korostynska, *Sens. Actuators, B* **2007**, *127*, 42.
- [82] R. P. Buck, *Anal. Chem.* **1974**, *46*, 28.
- [83] H. A. Zamani, M. Mohaddeszadeh, *Anal. Lett.* **2008**, *41*, 2710.
- [84] C. Puigo-Lleixa, C. Jimenez, E. Fabregas, J. Bartroli, *Sens. Actuators, B* **1998**, *49*, 211.
- [85] A. Eftekhari, *Sens. Actuators, B* **2003**, *88*, 234.
- [86] A. Cranny, N. R. Harris, M. Nie, J. A. Wharton, R. J. K. Wood, K. R. Stokes, *Sens. Actuators, A* **2011**, *169*, 288.
- [87] J. D. R. Thomas, *Pure Appl. Chem.* **2001**, *73*, 31.
- [88] M. Yuqing, C. Jianrong, F. Keming, J. Biochem. Biophys. Methods **2005**, *63*, 1.
- [89] J. Artigas, A. Beltran, C. Jiménez, A. Baldi, R. Mas, C. Domínguez, J. Alonso, *Comput. Electron. Agric.* **2001**, *31*, 281.
- [90] A. P. Soldatkin, D. V. Gorchkov, C. Martelet, N. Jaffrezic-Renault, *Sens. Actuators, B* **1997**, *43*, 99.
- [91] R. Bashir, A. Gupta, *Nanotechnology in Biology and Medicine*, CRC Press, Boca Raton, FL, USA **2007**.
- [92] H. F. Ji, K. M. Hansen, Z. Hu, T. Thundat, *Sens. Actuators, B* **2001**, *72*, 233.
- [93] C. Ruan, K. Zeng, C. A. Grimes, *Anal. Chim. Acta* **2003**, *497*, 123.
- [94] L. K. Sharma, A. A. Zaeen, S. K. Bali, J. D. Dwyer, in *Improving Nitrogen and Phosphorus Efficiency for Optimal Plant Growth and Yield* (Ed: Ö. Çelik), IntechOpen Limited, London, UK **2016**, p. 13.
- [95] D. L. Scarneccchia, F. Magdoff, *J. Range Manage.* **1994**, *47*, 315.

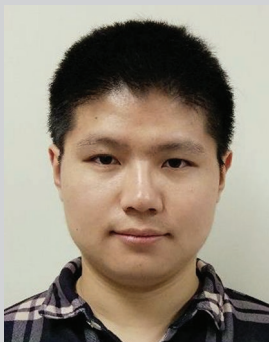
- [96] M. S. Guignard, A. R. Leitch, C. Acquisti, C. Eizaguirre, J. J. Elser, D. O. Hessen, P. D. Jeyasingh, M. Neiman, A. E. Richardson, P. S. Soltis, D. E. Soltis, C. J. Stevens, M. Trimmer, L. J. Weider, G. Woodward, I. J. Leitch, *Front. Ecol. Evol.* **2017**, *5*, 70.
- [97] L. Zhu, H. Jia, Y. Chen, Q. i. Wang, M. Li, D. Huang, Y. Bai, *Sensors* **2019**, *19*, 3417.
- [98] L. Lvova, M. Nadporozhskaya, in *New Pesticides and Soil Sensors* (Ed: A. M. Grumezescu), Elsevier Inc., New York **2017**, pp. 637–678.
- [99] R. S. Patkar, M. Ashwin, V. R. Rao, *Solid-State Electron.* **2017**, *138*, 94.
- [100] M. Razaq, P. Zhang, H. L. Shen, Salahuddin, *PLoS One* **2017**, *12*, e0171321.
- [101] D. P. Schachtman, R. Shin, *Annu. Rev. Plant Biol.* **2007**, *58*, 47.
- [102] K. A. Sudduth, J. W. Hummel, *Trans. ASAE* **1993**, *36.1*, 185.
- [103] K. A. Sudduth, J. W. Hummel, *Trans. ASAE* **1993**, *36.6*, 1571.
- [104] K. A. Sudduth, J. W. Hummel, *Proc. SPIE* **1993**, *1836*, 14.
- [105] J. D. Alexander, *Crops Soils* **1969**, *21*, 15.
- [106] P. Krishnan, J. D. Alexander, B. J. Butler, J. W. Hummel, *Soil Sci. Soc. Am. J.* **1980**, *44*, 1282.
- [107] R. C. Dalal, R. J. Henry, *Soil Sci. Soc. Am. J.* **1986**, *50*, 120.
- [108] B. Kuang, A. M. Mouazen, *Biosyst. Eng.* **2013**, *114*, 249.
- [109] J. M. Bremner, *J. Agric. Sci.* **1960**, *55*, 11.
- [110] R. B. Bradstreet, *Anal. Chem.* **1954**, *26*, 185.
- [111] P. L. Kirk, *Anal. Chem.* **1950**, *22*, 354.
- [112] N. T. Garland, E. S. McLamore, N. D. Cavallaro, D. Mendivelso-Perez, E. A. Smith, D. Jing, J. C. Claussen, *ACS Appl. Mater. Interfaces* **2018**, *10*, 39124.
- [113] J. Artigas, C. Jimenez, S. G. Lemos, A. R. A. Nogueira, A. Torre-Neto, J. Alonso, *Sens. Actuators, B* **2003**, *88*, 337.
- [114] O. V. Yagodina, E. B. Nikolskaya, N. B. Shor, *Anal. Chim. Acta* **2000**, *409*, 143.
- [115] V. I. Adamchuk, E. D. Lund, B. Sethuramasamyraja, M. T. Morgan, A. Dobermann, D. B. Marx, *Comput. Electron. Agric.* **2005**, *48*, 272.
- [116] M. A. Ali, X. Wang, Y. Chen, Y. Jiao, M. J. Castellano, J. C. Schnable, P. S. Schnable, L. Dong, in *2019 20th Int. Conf. on Solid-State Sensors, Actuators and Microsystems & Eurosensors XXXIII (TRANSDUCERS & EUROSENSORS XXXIII)*, IEEE, Piscataway, NJ, USA **2019**, pp. 170–173, <https://doi.org/10.1109/TRANSDUCERS.2019.8808341>.
- [117] S. J. Birrell, J. W. Hummel, *Comput. Electron. Agric.* **2001**, *32*, 45.
- [118] R. R. Price, J. W. Hummel, S. J. Birrell, I. S. Ahmad, *Trans. ASAE* **2003**, *46*, 601.
- [119] T. H. Gieling, G. van Straten, H. J. J. Janssen, H. Wouters, *Sens. Actuators, B* **2005**, *105*, 74.
- [120] M. Yokota, T. Okada, I. Yamaguchi, *Meas. Sci. Technol.* **2007**, *18*, 2197.
- [121] N. F. Hartman, J. L. Walsh, D. P. Campbell, U. Akki, *Proc. SPIE* **1995**, *2345*, 314.
- [122] R. Tang, Y. Shi, Z. Hou, L. Wei, *Sensors* **2017**, *17*, 882.
- [123] W. Ju, *Multiplexed Carbon Nanotube Sensing film for Smart Soil Application*, University of Washington Libraries, Tacoma, WA, USA **2019**.
- [124] L. A. Panes-Ruiz, M. Shayan, Y. Fu, Y. e. Liu, V. Khavrus, S. Oswald, T. Gemming, L. Baraban, V. Bezugly, G. Cuniberti, *ACS Sens.* **2018**, *3*, 79.
- [125] N. R. Kitchen, K. A. Sudduth, S. T. Drummond, P. C. Scharf, H. L. Palm, D. F. Roberts, E. D. Vories, *Agron. J.* **2010**, *102*, 71.
- [126] W. R. Raun, J. B. Solie, G. V. Johnson, M. L. Stone, R. W. Mullen, K. W. Freeman, W. E. Thomason, E. V. Lukina, *Plant Soil* **2002**, *820*, 815.
- [127] K. F. Bronson, T. T. Chua, J. D. Booker, J. W. Keeling, R. J. Lascano, *Soil Sci. Soc. Am. J.* **2003**, *67*, 1439.
- [128] T. T. Chua, K. F. Bronson, J. D. Booker, J. W. Keeling, A. R. Mosier, J. P. Bordovsky, R. J. Lascano, C. J. Green, E. Segarra, *Soil Sci. Soc. Am. J.* **2003**, *67*, 1428.
- [129] T. M. Shaver, R. Khosla, D. G. Westfall, *Precis. Agric.* **2011**, *12*, 892.
- [130] A. K. Tilling, G. J. O'leary, J. G. Ferwerda, S. D. Jones, G. J. Fitzgerald, D. Rodriguez, R. Belford, *Field Crops Res.* **2007**, *104*, 77.
- [131] A. Amtmann, J. P. Hammond, P. Armengaud, P. J. White, *Adv. Bot. Res.* **2005**, *43*, 209.
- [132] M. R. Maleki, L. Van Holm, H. Ramon, R. Merckx, J. De Baerdemaeker, A. M. Mouazen, *Biosyst. Eng.* **2006**, *95*, 425.
- [133] I. Bogrekci, W. S. Lee, *Biosyst. Eng.* **2005**, *92*, 527.
- [134] D. Jung, H.-J. Kim, H. S. Kim, J. Choi, J. D. Kim, S. H. Park, *Sensors* **2019**, *19*, 2596.
- [135] S. G. Lemos, E. A. Menezes, F. S. Chaves, A. R. A. Nogueira, A. Torre-Neto, A. Parra, J. Alonso, *Commun. Soil Sci. Plant Anal.* **2009**, *40*, 1282.
- [136] Z. Zou, J. Han, A. Jang, P. L. Bishop, C. H. Ahn, *Biosens. Bioelectron.* **2007**, *22*, 1902.
- [137] I. Bogrekci, W. S. Lee, in *2005 American Society of Agricultural Engineers (ASAE) Annu. Int. Meet.*, American Society of Agricultural and Biological Engineers, St. Joseph, MI, USA **2005**, p. 051040.
- [138] I. B. Won Suk Lee, *US20070013908A1*, **2007**.
- [139] M. M. Grand, G. S. Clinton-Bailey, A. D. Beaton, A. M. Schaap, T. H. Johengen, M. N. Tamburri, D. P. Connelly, M. C. Mowlem, E. P. Achterberg, *Front. Mar. Sci.* **2017**, *4*, 255.
- [140] F. E. Legiret, V. J. Sieben, E. M. S. Woodward, S. K. Abi Kae Bey, M. C. Mowlem, D. P. Connelly, E. P. Achterberg, *Talanta* **2013**, *116*, 382.
- [141] Soil Pests: Grubs, Gnats, <https://greenmethods.com/soil-pests/> (accessed: June 2020).
- [142] M. Cardim Ferreira Lima, M. E. Damascena de Almeida Leandro, C. Valero, L. C. Pereira Coronel, C. O. Gonçalves Bazzo, *Agriculture* **2020**, *10*, 161.
- [143] P. J. Vittum, *Insecticide Series, Part VII : Insect Monitoring Techniques and Setting Thresholds*, TurfGrass Trends, Cleveland, OH, USA **1997**.
- [144] PMA, PEST MONITORING and Group Presentation, **2013**.
- [145] I. Potamitis, I. Rigakis, N. Vidakis, M. Petousis, M. Weber, *J. Sens.* **2018**, *2018*, 3949415.
- [146] R. W. Mankin, D. W. Hagstrum, M. T. Smith, A. L. Roda, M. T. K. Kairo, *Am. Entomol.* **2011**, *57*, 30.
- [147] F. E. Lutz, *Insect Sounds, Bulletin of the AMNH*, American Museum of Natural History, New York **1924**.
- [148] A. E. Emerson, R. C. Simpson, *Science* **1929**, *69*, 648.
- [149] G. M. Sessler, J. E. West, *J. Acoust. Soc. Am.* **1962**, *34*, 1787.
- [150] R. Mankin, J. Fisher, in *Proc. Fourth Symp. Agroacoustics* (Ed: USDA-ARS), Acoustical Society of America, Melville, NY, USA **2002**, p. 152.
- [151] R. W. Mankin, J. Brandhorst-Hubbard, K. L. Flanders, M. Zhang, R. L. Crocker, S. L. Lapointe, C. W. McCoy, J. R. Fisher, D. K. Weaver, *J. Econ. Entomol.* **2009**, *93*, 1173.
- [152] D. Shuman, J. A. Coffelt, K. W. Vick, R. W. Mankin, *J. Econ. Entomol.* **1993**, *86*, 933.
- [153] D. W. Hagstrum, P. W. Flinn, D. Shuman, *J. Econ. Entomol.* **1996**, *89*, 211.
- [154] R. W. Mankin, J. R. Fisher, in *Proc. North American Root Weevil Workshop* (Ed: R. Rosetta), North Willamette Research & Extension Center, Aurora, OR, USA **2001**.
- [155] C. M. Görres, D. Chesmore, *Sci. Rep.* **2019**, *9*, 10115.
- [156] J. H. T. Luong, M. Habibi-Rezaei, J. Meghraoui, C. Xiao, K. B. Male, A. Karne, *Anal. Chem.* **2001**, *73*, 1844.
- [157] Y. Lan, Y. Huang, D. E. Martin, W. C. Hoffmann, *Appl. Eng. Agric.* **2009**, *25*, 607.
- [158] J. R. K. Lehmann, F. Nieberding, T. Prinz, C. Knoth, *Forests* **2015**, *6*, 594.

- [159] E. Puiga, F. Gonzalez, G. Hamilton, P. Grundy, in *Proc. MODSIM2015, 21st Int. Congress on Modelling and Simulation* (Eds: T. Weber, M. J. McPhee, R. S. Anderssen), Modelling and Simulation Society of Australia and New Zealand, Broadbeach, Queensland, Australia **2015**, pp. 10–15.
- [160] R. Hussain, P. Chawla, *Int. J. Adv. Res. Comput. Sci.* **2015**, 6, 129.
- [161] F. Hahn, *Algorithms* **2009**, 2, 301.
- [162] *Precision Crop Protection – The Challenge and Use of Heterogeneity* (Eds: E.-C. Oerke, R. Gerhards, G. Menz, R. A. Sikora), Springer, **2010**.
- [163] A. Antonacci, F. Arduini, D. Moscone, G. Palleschi, V. Scognamiglio, *TrAC, Trends Anal. Chem.* **2018**, 98, 95.
- [164] N. M. Bakhori, N. A. Yusof, A. H. Abdullah, M. Z. Hussein, *Biosensors* **2013**, 3, 419.
- [165] Y. Zhao, L. Liu, D. Kong, H. Kuang, L. Wang, C. Xu, *ACS Appl. Mater. Interfaces* **2014**, 6, 21178.
- [166] S. Siddiquee, K. Rovina, N. A. Yusof, K. F. Rodrigues, S. Suryani, *Sens. Bio-Sensing Res.* **2014**, 2, 16.
- [167] I. A. Mirsal, *Soil Pollution. Origin, Monitoring and Remediation*, 2nd ed., Springer-Verlag, Berlin/Heidelberg, Germany **2004**.
- [168] P. Rajkumar, T. Ramprasad, G. S. Selvam, in *New Pesticides and Soil Sensors* (Ed: A. M. Grumezescu), Elsevier Inc., New York **2017**, pp. 437–481.
- [169] A. Desaules, S. Ammann, P. Schwab, *J. Plant Nutr. Soil Sci.* **2010**, 173, 525.
- [170] R. G. Kaniressy, G. K. Sims, *Appl. Environ. Soil Sci.* **2011**, 2011, 1687.
- [171] B. B. Prasad, D. Jauhari, M. P. Tiwari, *Biosens. Bioelectron.* **2014**, 59, 81.
- [172] J. Dong, X. Wang, F. Qiao, P. Liu, S. Ai, *Sens. Actuators, B* **2013**, 186, 774.
- [173] L. Tang, G.-M. Zeng, G.-L. I. Shen, Y.-P. Li, Y. I. Zhang, D.-L. Huang, *Environ. Sci. Technol.* **2008**, 42, 1207.
- [174] D. E. H. Baskeyfield, F. Davis, N. Magan, I. E. Tothill, *Anal. Chim. Acta* **2011**, 699, 223.
- [175] M. Giannetto, E. Urmiltà, M. Careri, *Anal. Chim. Acta* **2014**, 806, 197.
- [176] V. Sacks, I. Eshkenazi, T. Neufeld, C. Dosoretz, J. Rishpon, *Anal. Chem.* **2000**, 72, 2055.
- [177] J. H. Lee, M. H. Oh, J. Park, S. H. Lee, K. H. Ahn, *J. Hazard. Mater.* **2003**, 105, 83.
- [178] Y. L. Hung, T. M. Hsiung, Y. Y. Chen, Y. F. Huang, C. C. Huang, *J. Phys. Chem. C* **2010**, 114, 16329.
- [179] J. Cooper, J. A. Bolbot, S. Saini, S. J. Setford, *Water, Air, Soil Pollut.* **2007**, 179, 183.
- [180] M. F. M. Noh, I. E. Tothill, *Anal. Bioanal. Chem.* **2006**, 386, 2095.
- [181] M. F. Mohd, R. O. Kadara, I. E. Tothill, *Anal. Bioanal. Chem.* **2005**, 382, 1175.
- [182] P. R. M. Silva, M. A. E. I Khakani, M. Chaker, A. Dufresne, F. Courchesne, *Sens. Actuators, B* **2001**, 76, 250.
- [183] T. Nedeltcheva, M. Atanassova, J. Dimitrov, L. Stanislavova, *Anal. Chim. Acta* **2005**, 528, 143.
- [184] I. Palchetti, S. Laschi, M. Mascini, *Anal. Chim. Acta* **2005**, 530, 61.
- [185] C. M. McGraw, T. Radu, A. Radu, D. Diamond, *Electroanalysis* **2008**, 20, 340.
- [186] D. Wilson, M. de los Ángeles Arada, S. Alegret, M. del Valle, *J. Hazard. Mater.* **2010**, 181, 140.
- [187] A. Abbaspour, E. Mirahmadi, A. Khalafi-nejad, S. Babamohammadi, *J. Hazard. Mater.* **2010**, 174, 656.
- [188] M. N. Kopylovich, K. T. Mahmudov, A. J. L. Pombeiro, *J. Hazard. Mater.* **2011**, 186, 1154.
- [189] A. K. Singh, M. K. Sahani, K. R. Bandi, A. K. Jain, *Mater. Sci. Eng. C* **2014**, 41, 206.
- [190] H. Wan, Q. Sun, H. Li, F. Sun, N. Hu, P. Wang, *Sens. Actuators, B* **2015**, 209, 336.
- [191] M. M. Mentele, J. Cunningham, K. Koehler, J. Volckens, C. S. Henry, *Anal. Chem.* **2012**, 84, 4474.
- [192] E. J. Maxwell, A. D. Mazzeo, G. M. Whitesides, *MRS Bull.* **2013**, 38, 309.
- [193] P. Rattanarat, W. Dungchai, D. Cate, J. Volckens, O. Chailapakul, C. S. Henry, *Anal. Chem.* **2014**, 86, 3555.
- [194] S. Magrisso, Y. Erel, S. Belkin, *Microb. Biotechnol.* **2008**, 1, 320.
- [195] X. Wang, X. Lu, J. Chen, *Anal. Chem.* **2014**, 2, 25.
- [196] X. Wang, M. Liu, X. Wang, Z. Wu, L. Yang, S. Xia, L. Chen, J. Zhao, *Biosens. Bioelectron.* **2013**, 41, 557.
- [197] R. Ilangoian, D. Daniel, A. Krastanov, C. Zachariah, R. Elizabeth, *Biotechnol. Biotechnol. Equip.* **2006**, 20, 184.
- [198] C. Chouteau, S. Dzyadevych, J. M. Chovelon, C. Durrieu, *Biosens. Bioelectron.* **2004**, 19, 1089.
- [199] O. O. Soldatkin, I. S. Kucherenko, V. M. Pyeshkova, A. L. Kukla, N. Jaffrezic-Renault, A. V. El'skaya, S. V. Dzyadevych, A. P. Soldatkin, *Bioelectrochemistry* **2012**, 83, 25.
- [200] Q. Hou, A. Ma, T. Wang, J. Lin, H. Wang, B. Du, X. Zhuang, G. Zhuang, *Anal. Bioanal. Chem.* **2015**, 407, 6865.
- [201] A. Ivask, M. François, A. Kahru, H.-C. Dubourgier, M. Virta, F. Douay, *Chemosphere* **2004**, 55, 147.
- [202] L. Xian-Gui, H. Wei, H. Cheng, M. Ting, Z. Wen-Hui, *Appl. Microbiol. Biotechnol.* **2010**, 87, 981.
- [203] P. Liu, Q. Huang, W. Chen, *Environ. Pollut.* **2012**, 164, 66.
- [204] C. Coelho, R. Branco, T. Natal-da-Luz, J. P. Sousa, P. V. Morais, *Chemosphere* **2015**, 128, 62.
- [205] D. Futra, L. Y. Heng, A. Ahmad, S. Surif, T. L. Ling, *Sensors* **2015**, 15, 12668.
- [206] S. M. Z. Hossain, J. D. Brennan, *Anal. Chem.* **2011**, 83, 8772.
- [207] I. Wilson, *Bioanalysis* **2017**, 9, 1.
- [208] A. Howell, C. Tucker, E. E. Grote, M. Veste, J. Belnap, G. Kast, B. Weber, S. C. Reed, *J. Vis. Exp.* **2019**, 2019, e60308.
- [209] S. Oren, H. Ceylan, P. S. Schnable, L. Dong, *Adv. Mater. Technol.* **2017**, 2, 1700223.
- [210] J. M. Nassar, S. M. Khan, D. R. Villalva, M. M. Nour, A. S. Almuslem, M. M. Hussain, *npj Flexible Electron.* **2018**, 2, 24.
- [211] M. Mzuku, R. Khosla, R. Reich, *Commun. Soil Sci. Plant Anal.* **2015**, 46, 1668.
- [212] Aqeel-Ur-Rehman, A. Z. Abbasi, N. Islam, Z. A. Shaikh, *Comput. Stand. Interfaces* **2014**, 36, 263.
- [213] A. Zerger, R. A. Viscarra Rossel, D. L. Swain, T. Wark, R. N. Handcock, V. A. J. Doerr, G. J. Bishop-Hurley, E. D. Doerr, P. G. Gibbons, C. Lobsey, *Int. J. Appl. Earth Obs. Geoinf.* **2010**, 12, 303.
- [214] A. Awasthi, S. R. N. Reddy, *Global J. Comput. Sci. Technol.* **2013**, 13, 23.
- [215] H. R. Bogena, J. A. Huisman, H. Meier, U. Rosenbaum, A. Weuthen, *Vadose Zone J.* **2009**, 8, 755.
- [216] H. R. Bogena, M. Herbst, J. A. Huisman, U. Rosenbaum, A. Weuthen, H. Vereecken, *Vadose Zone J.* **2010**, 9, 1002.
- [217] M. C. Vuran, I. F. Akyildiz, *Phys. Commun.* **2010**, 3, 245.
- [218] R. Cardell-Oliver, M. Kranz, K. Smettem, K. Mayer, *Int. J. Distrib. Sens. Networks* **2005**, 1, 149.
- [219] M. E. Bayrakdar, *IEEE Sens. J.* **2019**, 19, 10892.
- [220] A. Terzis, R. Musaloiu-E., J. Cogan, K. Szlavecz, A. Szalay, J. Gray, S. Ozer, C. J. M. Liang, J. Gupchup, R. Burns, *Int. J. Sens. Networks* **2010**, 7, 53.
- [221] L. Xiao, L. Guo, in *2010 Int. Conf. on Computer and Communication Technologies in Agriculture Engineering*, IEEE, Piscataway, NJ, USA **2010**, pp. 89–92, <https://doi.org/10.1109/CCTAE.2010.5544354>.
- [222] P. Corke, P. Valencia, P. Sikka, T. Wark, L. Overs, in *Proc. 4th Workshop on Embedded Networked Sensors, EmNets '07* (Ed. C. J. Sreenan), Association for Computing Machinery, New York, NY, USA **2007**, pp. 33–37, <https://dl.acm.org/doi/proceedings/10.1145/1278972>.
- [223] R. R. Belu, in *2012 9th Int. Conf. on Communications (COMM)*, IEEE, Piscataway, NJ, USA **2012**, pp. 275–278, <https://doi.org/10.1109/ICComm.2012.6262614>.

- [224] T. Toba, A. Kitagawa, *J. Sens.* **2011**, *1*, 2011.,
- [225] M. Boada, A. Lazaro, R. Villarino, D. Girbau, *IEEE Sens. J.* **2018**, *18*, 5541.
- [226] M. Boada, A. Lazaro, R. Villarino, E. Gil, D. Girbau, 2018 48th European Microwave Conf. (EuMC), IEEE, Piscataway, NJ, USA **2018**, pp. 235–238, <https://doi.org/10.23919/EuMC.2018.8541569>.
- [227] K. A. A. Makinwa, A. Baschirotto, P. Harpe, *Low-Power Analog Techniques, Sensors for Mobile Devices, and Energy Efficient Amplifiers*, Springer, Cham, Switzerland **2019**.
- [228] Y. H. Tsao, R. A. Husain, Y.-J. Lin, I. Khan, S.-W. Chen, Z.-H. Lin, *Nano Energy* **2019**, *62*, 268.
- [229] Y. Yang, H. Zhang, G. Zhu, S. Lee, Z.-H. Lin, Z. L. Wang, *ACS Nano* **2013**, *7*, 785.
- [230] T. H. Kwan, X. Wu, Q. Yao, *Appl. Energy* **2018**, *222*, 410.
- [231] H. Anandakumar, R. Arulmurugan, *Computational Intelligence and Sustainable Systems*, Springer, Cham, Switzerland **2019**.
- [232] H. M. Jawad, R. Nordin, S. K. Gharghan, A. M. Jawad, M. Ismail, *Sensors* **2017**, *17*, 1781.
- [233] P. Spachos, S. Gregori, *IEEE Internet Comput.* **2019**, *23*, 8.
- [234] D. Thakur, Y. Kumar, A. Kumar, P. K. Singh, *Wireless Pers. Commun.* **2019**, *107*, 471.
- [235] M. H. Wong, J. P. Giraldo, S.-Y. Kwak, V. B. Koman, R. Sinclair, T. T. S. Lew, G. Bisker, P. Liu, M. S. Strano, *Nat. Mater.* **2017**, *16*, 264.
- [236] C. H. Huang, G. P. Singh, S. H. Park, N.-H. Chua, R. J. Ram, B. S. Park, *Front. Plant Sci.* **2020**, *11*, 663.
- [237] K. Lee, J. Park, M. I.-S. Lee, J. Kim, B. G. Hyun, D. J. Kang, K. Na, C. Y. Lee, F. Bien, J.-U. Park, *Nano Lett.* **2014**, *14*, 2647.
- [238] W. Tang, T. Yan, J. Ping, J. Wu, Y. Ying, *Adv. Mater. Technol.* **2017**, *2*, 2.
- [239] W. Tang, J. Wu, Y. Ying, Y. Liu, *Anal. Chem.* **2015**, *87*, 10703.
- [240] V. B. Koman, T. T. S. Lew, M. H. Wong, S.-Y. Kwak, J. P. Giraldo, M. S. Strano, *Lab Chip* **2017**, *17*, 4015.
- [241] J. J. Kim, L. K. Allison, T. L. Andrew, *Sci. Adv.* **2019**, *5*, eaaw0463.
- [242] S. Y. Kwak, M. H. Wong, T. T. S. Lew, G. Bisker, M. A. Lee, A. Kaplan, J. Dong, A. T. Liu, V. B. Koman, R. Sinclair, C. Hamann, M. S. Strano, *Annu. Rev. Anal. Chem.* **2017**, *10*, 113.
- [243] T. T. S. Lew, V. B. Koman, P. Gordiichuk, M. Park, M. S. Strano, *Adv. Mater. Technol.* **2020**, *5*, 1900657.
- [244] S. Baek, E. Jeon, K. S. Park, K. H. Yeo, J. Lee, *J. Microelectromech. Syst.* **2018**, *27*, 440.
- [245] Y. Cao, E. Lim, M. Xu, J. K. Weng, B. Marelli, *Adv. Sci.* **2020**, *7*, 1903551.
- [246] P. R. Miller, Microneedles as Wearable Sensors for Plants, No. SAND2018-1447C, Sandia National Lab. (SNL-NM), Albuquerque, NM, USA **2018**.
- [247] Y. Jiao, X. Wang, Y. Chen, M. J. Castellano, J. C. Schnable, P. S. Schnable, L. Dong, in *2019 20th International Conference on Solid-State Sensors, Actuators and Microsystems & Euroensors XXXIII (TRANSDUCERS & EUROSENSORS XXXIII)*, IEEE, Piscataway, NJ, USA **2019**, pp. 37–40, <https://doi.org/10.1109/TRANSDUCERS.2019.8808527>.
- [248] Opportunities for Sensors in Digital Farming, TechVision Analysis, Frost & Sullivan, San Antonio, TX, USA **2019**.
- [249] Global Soil Moisture Sensors Industry, Global Industry Analysis, Mzximize Market Research Pvt. Ltd., Pune, Maharashtra, India **2020**.
- [250] Soil Moisture Sensors: Global Markets to 2022, BCC Research **2018**.



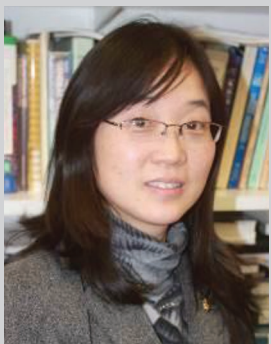
Heyu Yin is a Ph.D. student in the Department of Electrical and Computer Engineering, Michigan State University. He received his B.S. degree in engineering management from Hubei University, China and his Master's degree in microelectronics and nanoelectronics from Tsinghua University, China. His research interests are electrochemical sensors, microfluidics, and lab-on-CMOS integration for portable biosensing and environmental monitoring application.



Yunteng Cao is a Ph.D. candidate in civil and environmental engineering at Massachusetts Institute of Technology (MIT), supervised by Prof. Benedetto Marelli. He received his B.E. degree in engineering mechanics from Shanghai Jiao Tong University (China) in 2013 and his M.E. in solid mechanics from Xi'an Jiaotong University (China) in 2016. His research focuses on biopolymers and material delivery to plants and precision agriculture.



Benedetto Marelli received his Ph.D. in materials science and engineering from McGill University in 2012. He is currently the Paul M. Cook Career Development assistant professor at Massachusetts Institute of Technology. His research focus is on the design and nanomanufacturing of advanced biopolymers for applications in mitigation of environmental impact, food security, and precision agriculture.



Xiangqun Zeng is a distinguished professor at Department of Chemistry at Oakland University, USA. She obtained her Ph.D. in chemistry at State University of New York at Buffalo (SUNY Buffalo) in 1997. Her research focuses on electrochemistry and interface chemistry at solid electrodes, development of new analytical techniques, chemical and biosensors, ionic liquids, and conductive polymers. She is an Editorial Board member of *Journal of Electrochemistry*.



Andrew J. Mason received his B.S. in physics from Western Kentucky University in 1991, and his M.S. and Ph.D. in electrical engineering from The University of Michigan, Ann Arbor in 1994 and 2000, respectively. From 1999 to 2001, he was an assistant professor at the University of Kentucky. Since 2001 he has been with the Department of Electrical and Computer Engineering at Michigan State University, where he is currently a professor and a member of the Neuroscience Program and the Environmental Science and Policy Program.



Changyong Cao received his Ph.D. in mechanical engineering and materials science from the Australian National University in 2014, and then worked as a postdoctoral research associate at Duke University. He is currently an assistant professor in packaging, mechanical engineering, and electrical & computer engineering at Michigan State University, where he is directing the Laboratory for Soft Machines & Electronics. His research interests include soft materials, soft robotics, printable/flexible/stretchable electronics, energy harvesting and storage, and 3D/4D printing of multifunctional materials.